

Article

# Hybrid Renewable Energy Microgrid for a Residential Community: A Techno-Economic and Environmental Perspective in the Context of the SDG7

Nallapaneni Manoj Kumar <sup>1,\*</sup>, Shauhrat S. Chopra <sup>1,\*</sup>, Aneesh A. Chand <sup>2</sup>,  
Rajvikram Madurai Elavarasan <sup>3,\*</sup> and G.M. Shafiullah <sup>4,\*</sup>

<sup>1</sup> School of Energy and Environment, City University of Hong Kong, Kowloon, Hong Kong

<sup>2</sup> School of Engineering and Physics, The University of the South Pacific, Suva, Fiji; aneeshamitesh@gmail.com

<sup>3</sup> Department of Electrical and Electronics Engineering, Sri Venkateswara College of Engineering, Chennai 602117, Tamil Nadu, India

<sup>4</sup> Discipline of Engineering and Energy, Murdoch University, Murdoch 6150, Australia

\* Correspondence: mnallapan2-c@my.cityu.edu.hk or nallapanenichow@gmail.com (N.M.K.);

sschopra@cityu.edu.hk (S.S.C.); rajvikram787@gmail.com (R.M.E.); gm.shafiullah@murdoch.edu.au (G.M.S.)

Received: 30 March 2020; Accepted: 7 May 2020; Published: 12 May 2020



**Abstract:** Energy, being a prime enabler in achieving sustainable development goals (SDGs), should be affordable, reliable, sustainable, and modern. One of the SDGs (i.e., SDG7) suggests that it is necessary to ensure energy access for all. In developing countries like India, the progress toward SDG7 has somewhat stagnated. The aging conventional electric power system has its dominant share of energy from fossil fuels, plagued with frequent power outages, and leaves many un-electrified areas. These are not characteristics of a sustainable and modern system in the context of the SDG7. Promoting renewable-based energy systems, especially in the context of microgrids (MGs), is one of the promising advances needed to rejuvenate the progress toward the SDG7. In this context, a hybrid renewable energy microgrid (HREM) is proposed that gives assurance for energy access to all in an affordable, reliable, and sustainable way through modern energy systems. In this paper, a techno-economic and environmental modeling of the grid-independent HREM and its optimization for a remote community in South India are presented. A case of HREM with a proposed configuration of photovoltaic/wind turbine/diesel generator/battery energy storage system (PV/WT/DG/BESS) was modeled to meet the community residential electric load requirements. This investigation dealt with the optimum sizes of the different components used in the HREM. The results of this model presented numerous feasible solutions. Sensitivity analysis was conducted to identify the best solution from the four optimized results. From the results, it was established that a PV + DG + BESS based HREM was the most cost-effective configuration for the specific location. In addition, the obtained optimum solutions were mapped with the key criteria of the SDG7. This mapping also suggested that the PV + DG + BESS configuration falls within the context of the SDG7. Overall, it is understood that the proposed HREM would provide energy access to households that is affordable, reliable, sustainable, and modern.

**Keywords:** techno-economic modeling; environmental analysis; microgrid; community microgrid; hybrid renewable energy microgrid; energy access to all; SDG7

## 1. Background

Recently, sustainable development goals (SDGs) have generated much-needed discussions and research efforts, and in achieving these SDGs, the role of the energy sector seems to be crucial. Energy, being a prime enabler in achieving SDGs, should be affordable, reliable, sustainable, and modern.

One of the SDGs (i.e., SDG7) sets the target to ensure energy access for all [1]. Energy, especially electricity, is one of the main driving forces for a country's economic prosperity. Ensuring energy access to all in the context of the SDG7 would enable energy sustainability. However, at present, the significant share of the national energy mix in most countries is composed of fossil fuels. Countries strive deliberately to minimize the use of fossil fuels to attain sustainability in the energy sector. Over the years, the energy sector has also become more interested and sympathetic to the use of renewable energy resources (RERs) to meet energy demand. There are different types of RERs (e.g., solar, wind, biomass, tidal, wave, geothermal, etc.), and hydropower is also considered to be one of the RERs. On a global level, the use of RERs is gaining attention, and many countries (e.g., China, United States, Japan, India, Germany, Netherlands, etc.) are in favor of the deployment of renewables in the energy sector, seen in Figure 1. The global trend for investment in the renewable energy (RE) sector in various countries is shown in Figure 1a [2]. Promoting renewable energy systems, primarily through microgrids (MGs) seems to be one of the potential approaches to enable progress towards the SDG7. RERs-based MGs present a feasible solution to counterbalance the issues of depleting fossil fuel, environmental protection, and energy access. Also, the RERs-based energy systems have low carbon emissions and, overall, help in minimizing global warming.

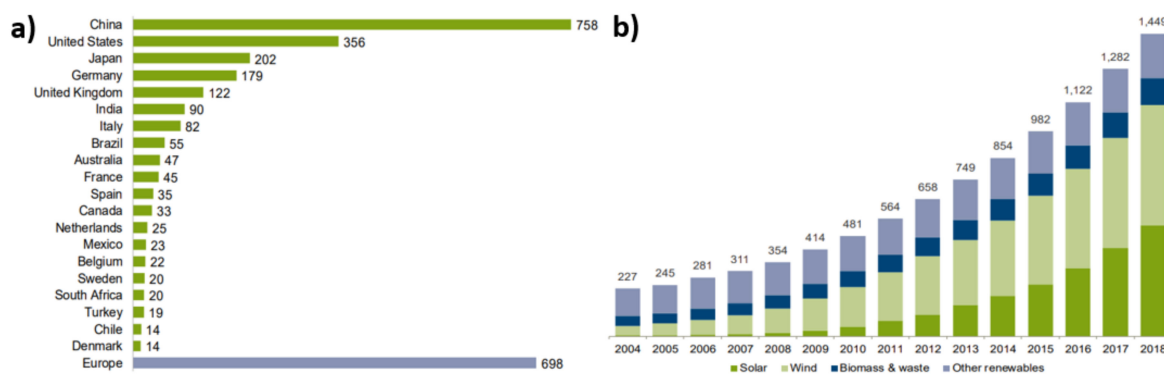


**Figure 1.** (a) Renewable energy capacity investment by various countries from 2010 to the first half of 2019, in United States Dollar (\$) billions; (b) Global capacity in renewable power from 2004–2018 in gigawatt (GW) [2].

Due to the recent surge in investments for renewable energy (RE) projects, the contribution of renewable power within the energy mix is also starting to pick up on a global level. A few countries are performing well and are leading the global RE installations. From the year 2010 to the first half of 2019, China invested around 758 billion USD, whereas Europe's investment was only 698 billion USD [2]. India stood in the sixth position in RE investments, with about 90 billion USD. The investments towards RE projects by other nations are also in the acceptable range as per their energy budget allocations. Currently, the worldwide share of RE is 11%, and it is expected to increase by 60% by 2070 [2]. As pointed out earlier, there are different RERs, and their contributions vary. Not all RERs have an equal share in terms of global installed power capacities. However, only a few RERs contribute to a significant share. Among all the RE systems, solar and wind have higher installed capacities. Solar energy can be harvested using thermal collectors as well as photovoltaic (PV) devices. Comparing solar thermal and PV, the use of solar PV has become more popular due to its promising benefits in terms of installation and capital investments. Besides, not all weather conditions are favorable for solar thermal installations, so their installation capacities are limited to 6451 megawatt (MW) [2]. As of September 2019, the installed capacity of solar photovoltaic (PV) alone increased by 26 times when compared to the 2009 capacity [2]. The global, solar PV and wind energy installations by the end of 2018 were 591.55 GW and 509 GW, respectively [2]. In Figure 1b, the global renewable power capacity in GW is given, and it is evident that the share of solar and wind power installations is increasing at a faster pace across the globe when compared to other RERs.

Considering the RE installations in India, as of December 2019, India has a total share of ~80 GW of RERs in its total installed capacity of 368.79 GW [3]. Out of that 80 GW, the solar energy share is 29.55 GW, and the wind energy share is 36.37 GW. Currently, the government has set a goal to increase its dependence on renewables to 175 GW by 2022 to limit fossil fuel use. In addition, targets for solar and wind installation were set by the government, and they are 100 GW and 60 GW, respectively [4]. In addition to the set targets, there has been a remarkable increase recently in investments and the implementation of policies to promote solar energy and biomass use and to raise awareness about other RERs [5]. Even though India is doing well in terms of energy investments and policies, ensuring energy access for all is becoming difficult. At present, in India, only 84.5% of the population has access to electricity, out of which around 41% have access to clean fuels [6]. Within the context of the SDG7, ensuring energy access for all is emphasized, and energy should be affordable, reliable, sustainable, and modern. However, in India, the achievement of the SDG7 is more or less stagnant, and the reasons for this are a fossil-fuels-dominant national energy mix, frequent power outages, and many unelectrified areas. As per the 2019 statistics, the SDG7 score of India was at 65.4, which is quite low when compared to many other developing countries [6]. In Figure 2, the progress of the SDG7 on a global level is presented, which reveals that India falls under the red zone and indicates that there exist significant challenges.

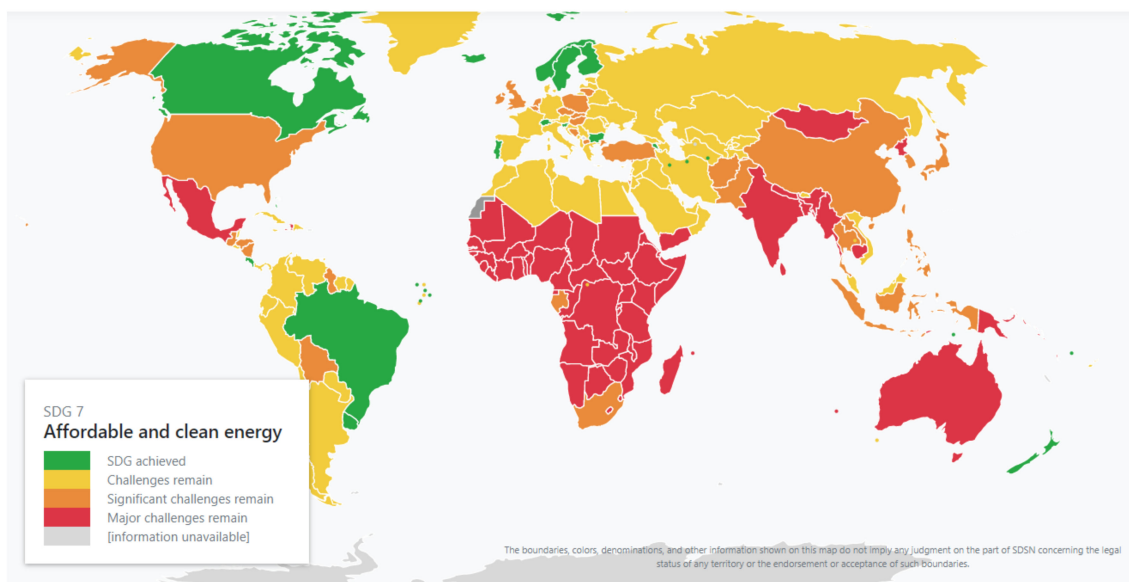


**Figure 2.** Map showing the progress of sustainable development goal 7 (SDG7) “affordable and clean energy” across the globe [6].

India’s energy sector is dominated by fossil fuels, mainly coal and oil. As per the 2019 statistics, the shares of coal, oil, gas, hydro, nuclear, and renewables in the energy mix are 55.9%, 0.1%, 6.9%, 12.4%, 1.9%, and 23.5%, respectively [3]. As per the British Petroleum (BP) energy outlook in 2019, the percentage of coal was reduced to 48%. On the other hand, gas consumption for power generation increased by 2%, and hydro was reduced by 1%. There was a slight increment seen in nuclear, i.e., 1%. However, the renewables share increased from 3% to 16% [7]. Comparing the predicted statistics of BP energy with the current scenarios reveals that India’s energy sector is progressing in increasing non-fossil fuel energy. The statistics related to the energy mix suggest that the accessed energy by the people in India is not sustainable as it is mostly coming from fossil fuels. Moreover, India still has issues with electrification. The reliability of the current power system is very poor. Over the last decade, power outages have become an everyday reality. However, the major outage was the one that happened in July 2012, which resulted in blackouts causing no power supply to 700 million people as per the Guardian article [8]. The power outage was due to the failure seen in the northern grid, that cascaded to the eastern grid, and then the northeastern grid. It is estimated that 20 out of 28 states in

India were affected by these power outages. With all these issues, achieving the SDG7 is a significant but worthy challenge for India.

India is striving deliberately to minimize the energy share of fossil fuels in its national energy mix, hoping to attain sustainability in the energy sector by focusing on the targets of the SDG7. The BP energy outlook 2019 report says that the projected share in primary energy consumption in India in 2040 will concentrate more on renewables deployment, giving scope for achieving the SDG7 [7]. India realized the importance of promoting renewables-based energy systems, but the implementation of such systems is a challenging task when taking into account the intermittent existence of RERs and multi-dimensional design aspects. For those areas where the use of conventional grid electricity cannot be made possible or where network expansion costs are relatively high, the use of RERs is generally suggested. RERs such as solar, wind, small hydro, and bioenergy are an appealing option, especially for rural electrification in India. The major difficulty with using these renewable power systems is that due to the intermittent nature of these resources, they cannot provide reliable electricity [9]. To overcome this, energy storage systems (ESSs), such as a battery banks, flywheels, pumped storage, supercapacitors are used for better reliability. Such devices are usually used for large-capacity networks and require high capital investment, but they can be implemented to achieve a reliable electricity supply even under the worst conditions of RERs [9,10]. Among the possible ESSs, the battery energy storage system (BESS) is widely deployed [9].

Therefore, a combination of RERs with BESS could be a promising off-grid energy system, not only in the Indian context but also globally. Increased interest in the use of small-scale hybrid energy sources in power distribution networks has contributed to the introduction of microgrids (MGs) in recent years. Hence, the concept of a microgrid is identified as a better solution for rural electrification, and different hybrid MG configurations of RERs are presented in the literature [11,12]. MGs are considered the most reliable, stable, cost-effective, and environmentally friendly energy option [11]. A localized electrical system that can operate autonomously and deliver power to the community or household can be an MG [10]. While planning for an MG, there are a few intermittent characteristics to be considered: These include power quality and voltage from an electrical perspective. Hence, considering these are essential while planning MGs [11,12]. The availability of abundant RERs in India provides a high possibility of harnessing these sources as an alternative for remote area electrification [10–13]. The energy conversion systems like PV, and wind turbine (WT) can be used in combination by making hybrid configurations, especially MGs or hybrid renewable energy systems (HRES). These hybrid configurations will improve system reliability and performance while decreasing fluctuations in the generation, investment costs, and storage system size [11,13]. During the grid-independent operation, the off-grid hybrid system may not be able to support the full load; therefore, ESSs provide the backup energy needs during conditions of variable output power from the RERs [13–17]. ESSs integration in the HRES reduces the overall cost and improves resilience of the system [15,17]. In addition, the reliability of the HRES is also ensured by its delivery of continuous power to the load [17,18]. In some cases, the use of a diesel generator (DG) is also encouraged to ensure continuous power to the load during the intermittent conditions of RERs. Policymakers and researchers have shown and proven that an optimal design of HRES can be used in power generation. In addition, promoting renewable-based energy systems, especially the MGs, seems to enable progress towards the SDG7. The renewables-based MGs can operate in an island mode and reduce the dependency on fossil fuel. Besides which, they have important economic and environmental benefits [18]. Hence, hybrid renewable energy microgrids (HREM) based on localized RERs and BESS should be better options for meeting the energy demands of load centers. In this context, we propose a HREM that gives assurance for energy access to all in an affordable, reliable, sustainable way through modern energy systems.

In this paper, techno-economic-environmental modeling and optimization of grid-independent HREM for a remote community were proposed for a location in South India. A case of HREM with a proposed hybrid configuration of PV/WT/DG/BESS was modeled to meet the residential electric load requirements of the community. This investigation aimed to deal with the optimum sizes of the different

components used in the HREM. In other words, it formulated and identified the optimal system configuration of HREM for achieving techno-economic-environmental feasibility with a maximized renewable fraction and with the lowest net present cost and cost of electricity by using locally available RERs. Overall, the formulated scope of the study aimed to provide energy for all through HREM as per the SDG7, considering the critical aspects of energy, which include being affordable, reliable, sustainable, and modern.

This paper has four-section, Section 2 presents the literature review on the hybrid renewable energy system and the tools used for modeling such systems; in Section 3, modeling design and evaluation of HREM are given; in Section 4, framework and the optimization methodology that was used to optimize the HREM system components is explained. In Section 5, the load assessment, resource assessment, cost assessment, and data inputs required for modeling are discussed. In Section 6, the results are presented and discussed, and in Section 7, the conclusions are provided.

## 2. Literature Review

Extensive research has been done in the area of MGs, HRESs, and HREMs that include two or more RERs and EESs. In addition, there is ample literature showing the benefits and challenges associated with such HRES [12,15].

Hybrid optimization models were developed for Australia, Bangladesh, Busan, Maldives, and South Korea to maximize the electricity generation from RE resources through techno-economic feasibility analysis using the hybrid optimization model for multiple energy resources (HOMER) [19–24]. Panayiotou et al. [25] designed an optimal standalone PV system and an autonomous hybrid PV/WT system to examine the feasibility of implementing a standalone hybrid system in Nicosia, Cyprus, and Nice, France. Gangwar et al. [26] investigated the cost and reliability of different combinations of hybrid systems consisting of PV/WT/proton exchange membrane fuel cell (PEMFC)/BESS using HOMER software. Increasing energy demand and a sharp rise in fossil fuel prices in Bangladesh has led to an investigation of the PV/WT/DG system and its feasibility. The analysis showed a considerable reduction in CO<sub>2</sub>, which is of widespread concern in modern industrial life [27]. Similarly, in the interest of reducing fossil fuel consumption and minimizing emissions, Colantoni et al. [28] contributed a mathematical model for the potential of a hybrid PV/WT system. Ahmad et al. [29] used HOMER software to study a grid integrated hybrid system without any energy storage.

A considerable amount of work in HRES has evaluated and mathematically proven. Table 1 shows a summary of HRES research.

**Table 1.** Summary of the hybrid renewable energy systems (HRES) analyses for various applications.

Ref.	Descriptions
Baghdadi et al. [30]	Optimized a hybrid fossil-power system to ensure higher fuel saving while maximizing renewable electricity.
Enevoldsen and Sovacool [31]	An isolated microgrid energy system was designed for Faroe Islands using a storage system to increase its reliability.
[32]	Utilized particle swarm optimization-based simulation for HRES.
Biswas and Kumar [33]	An HRES was used for designing a PV/pumped hydro energy storage (PHES)/BESS system for an academic building of an engineering institution.
Fazelpour et al. [34]	In Kish Island, Iran, a feasibility study was carried out on various hybrid energy systems, including diesel generator, battery, wind system, and PV, to cover the electrical load of a hotel.

Table 1. Cont.

Ref.	Descriptions
Bhattacharjee and Acharya [35]	An HRES study was carried out in a northeastern city, Tripura, to show the low wind area for a small-scale educational building.
Türkay and Telli [36]	The analysis shows a better performance of grid-connected HRES than that of completely renewable configurations by exploring the grid-connected PV/WT/fuel cell (FC) system. In addition, the impacts of PV and hydrogen systems on the main grid were explored. The average solar radiation intensity and wind energy capacity of Istanbul projected a feasible solution.
Thakur et al. [37]	A hydropower project was deemed to be better than wind power in terms of its efficiency and reliability.
Nafeh [38]	A feasibility study on a photovoltaic PV/WT hybrid energy home system, incorporating a storage battery, was developed.
Li et al. [39]	The size optimization of a micro-grid based on the evolutionary algorithm was accomplished.
Abdelhamid and Rachid [40]	Techno-economical optimization was addressed for an isolated system (PV/WT/DG/BESS).
Heydari and Askarzadeh [41]	Sizing of an isolated system (PV/WT/DG/BESS) was minimized using a harmony search algorithm.
Spyrou and Anagnostopoulos [42]	A standalone HRES comprised of PV/WT/PHES for powering desalination plants was designed using a stochastic evolutionary algorithm, which reduced the actual water transportation cost by a significant amount.

A systematic discussion of RERs and their adoption is ongoing. Zahboune et al. [43] showed a theoretical and novel upgraded cascade approach model for an electric system designed using a PV/WT system based on power pinch analysis. They used HOMER software to analyze feasibility; a comparison study was presented with the results showing a difference of 0.07% in the cost of energy (COE), 5.4% in excess energy, and 0.04% in energy production. Five different configurations of HRES with a hydrogen-powered generator were studied for a residential application by Fazelpour et al. [44]. Their findings were based on the feasibility study of replacing DG; the reported result was the most economically viable for HRES with a configuration of WT/DG/BESS/electrolyzer. A techno-economic model was presented for the assessment of an HRES for a rural community across six locations in Nigeria by Oyedepo et al. [45]. They found during the analysis that the COE varied directly with the strength of the wind and solar irradiation received at the locations under study

Considerable research has been conducted for size optimization of off-grid or grid-independent MGs [46–53]. Studies have shown different off-grid or grid-independent HREMs. Table 2 provides the details regarding the research studies carried out on various HREM systems. The simulation platforms used for HREM modeling along with the HREM configuration, as well as their contribution or the main objectives, are presented.

From the above literature, it is understood that promoting HREM for meeting energy demands of various applications is a feasible option. In addition, for modeling and optimization of such HREMs, the HOMER optimization tool is widely used, and it is one of the available techniques as per industrial standards. However, to date in the literature, the studies have been mostly limited to individual household loads. These studies are mostly very straight forward and highlight the HREM feasibility by ensuring lower net present value (NPV) and COE. However, the studies in the context of SDGs are limited. To the authors' knowledge, feasibility studies of HREM using HOMER modeling and optimization in the context of the SDG7 are not available. We believe that there is a scope for understanding the HREM feasibility within the context of the SDG7.

**Table 2.** Summary of the recent literature on grid-independent hybrid renewable energy microgrids (HREMs) and their contributions.

Location	Year of the Study	Simulation Platform	Configuration Types	Contributions and Main Ideas	Reference
Oman	2019	HOMER	PV + BESS	Finding a suitable location to install the PV system to replace DG. Minimize carbon emissions. Lower NPC and COE.	Abdul-Wahab et al. [54]
Saudi Arabia	2019	HOMER	WT + BESS	Design 15 MW wind farms and carry out a techno-economic feasibility study. To see significant COE reduction.	Shaahid et al. [55]
Tunisia	2019	MATLAB	PV + FC + UC	Improve power security by involving an energy management strategy. Ensuring energy supply without interruption.  Detailed feasibility study and economic analysis of a hybrid energy system.	Sami et al. [56]
India	2019	MATLAB	PV + WT + BESS	Lower COE.	Das et al. [57]
China	2019	MATLAB	PV + WT + BESS	Mitigating the disharmony between load/generation balance, cost optimization, and saturation.	Ma and Javed [58]
Bangladesh	2020	HOMER	Biogas + EV	Feasibility study and economic analysis. Lower NPC and COE.	Karmaker et al. [59]

Note: HOMER-Hybrid optimization model for electric renewables; MATLAB-Matrix laboratory; PV-Photovoltaics; BESS-Battery energy storage system; WT-Wind turbine; FC-Fuel cell; UC-Ultra capacitor; EV-Electric vehicle; DG-Diesel generator; NPC-Net present cost; COE-Cost of electricity; MW-Megawatt.

Hence, a study was formulated to model an HREM for meeting the community electricity loads, and the key contributions of this study are as follows:

- A framework for hybrid energy system optimization was proposed by considering the key features of the SDG7, i.e., affordable, reliable, sustainable, and modern.
- Under each feature of the SDG7, a few indicators were identified, i.e., affordable: lower COE, NPV, and capital investments; reliable: continuous power supply, minimized energy shortage, and ensured quality of power; sustainable: higher renewable fraction and minimum emissions; and modern: MGs, hybrid power systems, and community MGs.
- Modeling of the HREM considering PV/WT/DG/BESS was designed and analyzed for a household community in South India by considering the weather conditions.
- Optimization of the HREM was carried out to select the best feasible configuration within the context of the SDG7 by considering explored indicators as constraints.

### 3. Description and Modeling of the Hybrid Renewable Energy Microgrid (HREM)

A schematic layout of the proposed HREM, shown in Figure 3, that was modeled and designed to satisfy the electric load demand of a remote household community is presented in this section.

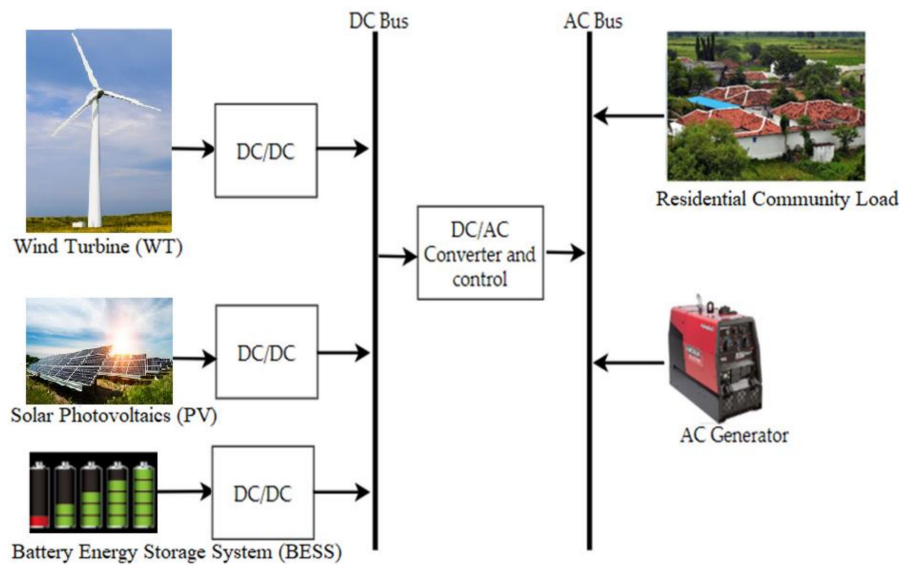


**Figure 3.** Schematic representation of the proposed hybrid renewable energy microgrid (HREM) for the remote household community. (Note: DC—Direct current; AC—Alternating current)

In the proposed configuration of the HREM, a PV, WT, DG, BESS, and power converter were used. Two different electric load buses were considered. The alternating current (AC) load bus was linked to DG, while the direct current (DC) load bus was linked to both the solar PV and WT systems by means of the power converter. In addition, BESS was also linked to the DC load bus. The solar PV and WT systems produce DC power, which is influenced by weather parameters. Hence a DC/DC power converter was used to regulate the power outputs. In the case of excess power generated from any of the power generating sources used in this HREM, that excess power was stored in the BESS. Whenever an energy shortage exists, the energy stored in the batteries can be used. The flow of energy from the generating units to electric loads through the power conversion systems can be seen visually in the schematic diagram of the HREM shown in Figure 3.

### 3.1. Solar Energy Conversion System (SECS)

In the proposed HREM, the PV module produces DC electricity in direct proportion to the incident solar radiation. However, the PV derating factor and the temperature have negative effects on the overall DC electricity produced. Therefore, the power output of the PV module can be calculated using the following Equation (1) [60]:

$$P_{PV} = W_{PV} f_{PV} \left[ \frac{G_T}{G_{STC}} \right] \left[ 1 - \alpha_p (T_c - T_{C,STC}) \right] \quad (1)$$

where  $W_{PV}$  is the peak power output of the PV module (kW),  $f_{PV}$  and  $\alpha_p$  are the PV derating factor (%) and power temperature coefficient, respectively,  $G_T$  is the solar radiation incident on the PV module in the current hour ( $\text{kW}/\text{m}^2$ ),  $G_{STC}$  is the incident radiation under standard test conditions ( $1 \text{ kW}/\text{m}^2$  at 25),  $T_c$  is the PV panel temperature ( $^{\circ}\text{C}$ ), and  $T_{C,STC}$  is the PV cell temperature under standard conditions ( $^{\circ}\text{C}$ ).

The energy balance equation for the PV system is given in Equation (2), and it is the function of ambient and PV cell temperatures. While the cell temperature can be obtained using Equation (3) [61].

$$\tau \alpha G_T = \eta_c G_T + U_L (T_c - T_a) \quad (2)$$

$$T_c = T_a + G_T \left( \frac{\tau \alpha}{U_L} \right) \left[ 1 - \frac{\eta_c}{\tau \alpha} \right] \quad (3)$$



where  $\tau(\%)$  is the transmittance of the cover over the PV array,  $\alpha(\%)$  is the solar absorptance of the PV array,  $\eta_c(\%)$  is the electrical conversion efficiency of the PV array,  $T_a(\text{C})$  is the ambient temperature, and  $U_L(\text{kW}/\text{m}^2\text{C})$  is the coefficient of heat transfer to the surroundings.

The PV array is based on the number of panels connected in series ( $N_s$ ) and parallel ( $N_p$ ) configuration, and their efficiency is calculated as, respectively, Equations (4) and (5) [61,62].

$$P_{PV, STC} = (N_s \times N_p) P_{mSTC} \quad (4)$$

$$\eta_{mp, STC} = \frac{P_{PV}}{A_{PV} G_{T,STC}} \quad (5)$$

### 3.2. Wind Energy Conversion System (WECS)

In the proposed HREM, the WECS is one of the power generating sources where the wind turbine converts the kinetic energy of the wind into DC or AC electricity depending upon the type of electrical machine used. The output power for a wind turbine is a function that is defined as shown in Equation (6) [62,63].

$$P_w(V) = \begin{cases} \frac{1}{(V_R^3 - V_C^3)} [V^3 - V_C^3] P_R, & V_C \leq V \leq V_R \\ P_R, & V_R \leq V \leq V_F \\ 0, & \text{elsewhere} \end{cases} \quad (6)$$

The power curve shown in Figure S1 gives a detailed understanding of the wind turbine power outputs in WECS. An ideal turbine has a mechanical power output ( $P_m$ ) given by the well-known Betz' Law for airspeeds as given in Equation (7) [60].

$$P_m = \frac{1}{2} C_p \rho A v^3 \quad (7)$$

where  $C_p$  is the power co-efficient,  $\rho$  is the air density,  $A$  is the cross-sectional area of wind or the swept area of the turbine blades, and  $v$  is the wind speed (m/s).

At a given location and height, the electric power output of the wind turbine depends on the wind speed at hub height and the turbine speed. The power-law equation of wind velocity at hub height can be expressed as given in Equation (8) [62,63]:

$$\frac{V(h)}{V(h_{ref})} = \left( \frac{h_h}{h_{ref}} \right)^x \quad (8)$$

where  $V(h)$  and  $V(h_{ref})$  are the wind velocities at hub height ( $h_h$ ) and reference height ( $h_{ref}$ ), respectively, and  $x$  is a roughness factor.

### 3.3. Battery Energy Storage System (BESS)

In a microgrid, ESS is primarily used to assist the HREM to have a stable and smooth operation and maintain a constant voltage in the event of a mismatch between generation and consumption of power, and as such, the use of BESS is essential for maximum utilization of the available RERs [64]. Batteries of the same rating are connected in series and parallel to acquire higher energy capacities and backup [65]. At the same time, charging or discharging are dependent on generation power and consumption power. In such a case, the input power of the batteries can be either positive or negative, depending on whether the battery bank is being charged or discharged. The state of charge (SoC) and the depth of discharge (DoD) can be evaluated, as shown in Equations (9) and (10) [63].

SoC:

$$E_{Bat}(t) = E_{Bat}(t-1)(1-\sigma) + \left[ E_{Gen}(t) - \frac{E_{Required}(t)}{\eta_{inv}} \right] \eta_B \quad (9)$$

DoD:

$$E_{Bat}(t) = E_{Bat}(t-1)(1-\sigma) - \left[ \frac{E_{Required}(t)}{\eta_{inv}} - E_{Gen}(t) \right] \quad (10)$$

where  $E_{Bat}(t)$  and  $E_{Bat}(t-1)$  are the energy stored in a battery bank (Wh) at hour  $t$  and  $t-1$ , respectively;  $\sigma$  is the hourly self-discharge rate;  $E_{Required}(t)$  is the hourly energy required by the load;  $\eta_{inv}$  and  $\eta_B$  are the efficiencies of the inverter and charge efficiency of the battery bank, respectively, and  $E_{Gen}(t)$  is the energy generated by the hybrid PV/wind system at hour  $t$ .  $E_{Gen}(t)$  is given by Equation (11) [63,64].

$$E_{Gen}(t) = N_{PV}E_{PV}(t) - N_W E_W(t) \quad (11)$$

where  $N_{PV}$  and  $N_W$  are the number of PV modules and wind turbines, respectively. While  $E_{PV}(t)$  and  $E_W(t)$  are the hourly energies produced by one PV module and one wind turbine, respectively.

At any time  $t$ , the charged quantity of the battery bank is subject to the following constraints, as shown in Equation (12) [63].

$$E_{Bat, min} \leq E_{Bat}(t) \leq E_{Bat, max} \quad (12)$$

where  $E_{Bat}(t)$  is the energy stored in the battery bank,  $E_{Bat, min}$  and  $E_{Bat, max}$  are the minimum and maximum energy stored in the battery bank, respectively.

The nominal capacity of the battery,  $P_{Bat}(t)$ , is the power exchange at time  $t$  based on the following Equation (13) [63].

$$P_{Bat}(t) = P_{PV}(t) + P_{WT}(t) + P_{Dig, generator}(t) - P_{load}(t) \quad (13)$$

### 3.4. Diesel Generator (DG)

The RERs have alternating output characteristics, integrating these with a utility grid usually limits the user-side demand. In general, DG is a fundamental element in designing a microgrid network, as it offers many benefits in terms of emergency standby power, system reliability, time-consuming power, prime power, and ongoing operating power [60,64]. Hence, the fuel consumption rate can be estimated by using a quadratic polynomial, as shown in Equation (14).

$$Fuel\ Consumption = \sum_{i=1}^n (a + bP_i + cP_i^2) \{ \$ / hr \} \quad (14)$$

where  $n$  is the number of diesel generators and  $a$ ,  $b$ , and  $c$  are the cost coefficients of the diesel generator.

### 3.5. Power Convertors

In the proposed HREM, based on the power generating units, power converters were modeled. Here, the power converter was essential to have a continuous flow of power between the system and the load. The AC and DC buses were linked through a DC-AC converter, the output power of which was determined considering the efficiency parameter of the power converter [60,64]. The converting device (inverter and rectifier to exchange DC to AC electricity and vice versa) associated with HOMER can be defined with its efficiency, as shown in Equations (15) and (16).

$$P_{inv, out} = \eta_{inv} P_{DC} \quad (15)$$

$$P_{rec, out} = \eta_{rec} P_{AC} \quad (16)$$

where  $P_{inv, out}$  is the power output from the inverter (kWh);  $P_{DC}$  is the DC power input from the DC bus to the inverter (kWh);  $P_{rec, out}$  is the rectified power output from the inverter to the battery (kWh); and  $P_{AC}$  is the power output from the AC bus (kWh).

### 4. Framework and the Optimization Methodology

For optimizing the proposed HREM, a well-structured framework was necessary. This framework should ensure that the power requirements of the remote households in a community are continuously met. In this study, a framework was proposed to design the HREM, and it was developed by considering the four critical features of the SGD7, see Figure 4.

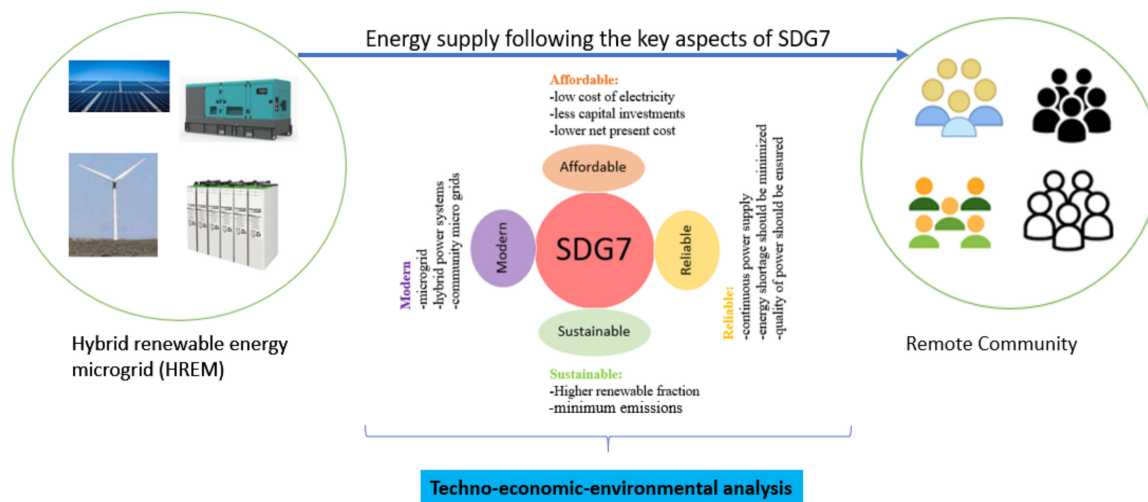


**Figure 4.** Framework for the hybrid renewable energy microgrid (HREM) in the context of sustainable development goal 7 (SDG7).

For each critical feature of the SDG7, a few indicators were identified, which were further used as constraints during optimization. These indicators included lower cost of energy (COE), net present value (NPV), and capital investments (for affordable); continuous power supply, minimized energy shortage, and ensured quality of power (for reliable); higher renewable fraction and minimum emissions (for sustainable); and MGs, hybrid power systems, community MGs (for modern). These identified indicators fall under three different analyses (technical, economic, and environmental). Hence, to model the HREM system within the context of the SDG7 demanded a techno-economic-environmental analysis.

In the HOMER simulation tool, a proposed HREM can be modeled; in fact, any of the conceptual MGs architectures can be modeled. The tool has many inbuilt power conversion devices, distributed energy resources, and other data that are required to model such systems. Based on the shown methodology in Figure 5, the modeling and optimization of the proposed HREM for meeting the community’s loads and sensitive cases were carried out. This involved pre-assessment to consider loads, resources, and system designs followed by sensitivity analysis with variation of the desired input parameters such as solar irradiance, wind speeds, discount rates, etc.

The methodology used to model the proposed HREM for a residential community within the context of the SDG7 is discussed further here and can be broadly divided into three main steps:

In the first step, the pre-assessment of loads, resources, and system design are done. Here, the selection of meteorological data as per the proposed HREM configuration is considered. For example, if the HREM configuration is based on WT and PV, then the selection of wind speed data and solar radiation data is essential, and it has to be done in the first step based on the study location using the pre-built data sets. In addition, a user can input their own monitored data. Once done, the load data of the remote households in a community should be given. Later, the selection of electric power components is generally made.

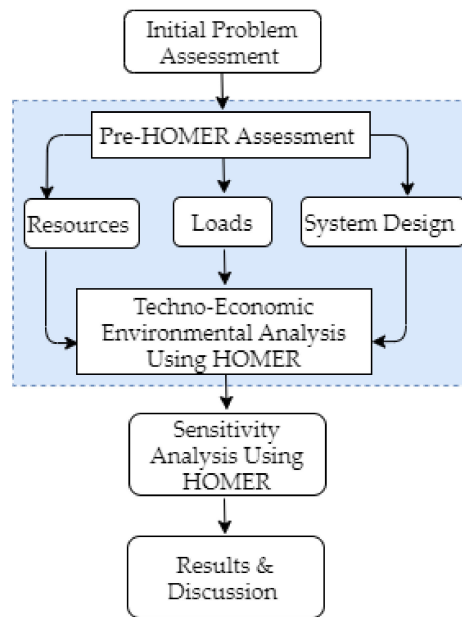


**Figure 5.** The methodology used for the techno-economic-environmental analysis of hybrid renewable energy microgrid (HREM). (Note: HOMER-Hybrid optimization model for electric renewables).

In the second step, the techno-economic and environmental analysis is carried out. While modeling each component of HREM, technical parameters, cost parameters, and optimum sizing search spaces are enabled along with specific constraints to achieve cost-effective HREM configuration. The renewable fraction generally represents the share of energy originated from RERs for meeting the load. The main reason for considering the renewable fraction is to ensure that the supplied energy is sustainable with less environmental emissions, which is one of the critical characteristics of the SDG7. The renewable fraction is estimated using Equation (17) [17].

$$f_{ren} = 1 - \frac{E_{nre} + H_{nrt}}{E_{es} + H_{ts}} \quad (17)$$

where  $f_{ren}$  is the renewable fraction and is expressed in %,  $E_{nre}$  is the electricity production from non-renewables in kWh/y,  $H_{nrt}$  is the non-renewable thermal production in kWh/y,  $E_{es}$  is the energy used to serve the electrical loads in kWh/y, and  $H_{ts}$  is the energy used to serve the thermal loads in kWh/y.

The identification of a cost-effective system is analyzed based on the following cost parameters.

Net present cost (NPC) indicates the installation cost and the operating and maintenance costs of the system throughout its lifetime, which is calculated by using Equation (18) [60,64].

$$NPC = \frac{TAC}{CRF(i, Rpr_j)} \quad (18)$$

where  $TAC$ ,  $CRF$ ,  $i$ , and  $Rpr_j$  are the total annualized cost (\$), capital recovery factor, the interest rate in percentage, and project lifetime in a year, respectively.

Total annualized cost is the sum of the annualized costs of all equipment of the power system, including capital and operation and maintenance costs. It also includes replacement and fuel costs [13].

Capital recovery factor is a ratio that is used to calculate the present value of a series of equal annual cash flows given by Equation (19) [60].

$$CRF = \frac{i \times (1 + i)^n}{(1 + i)^{n-1}} \quad (19)$$

where  $n$  and  $i$  represent the number of years and the annual real interest rate, respectively.

Annual real interest rate is a function of the nominal interest rate shown in Equation (20) [15].

$$i = \frac{i' - F}{1 + F} \quad (20)$$

where  $i$ ,  $i'$ , and  $F$  are the real interest rate, nominal interest rate, and annual inflation rate, respectively.

Cost of energy (COE) is the average cost/kWh of useful electrical energy produced by the system. The COE is calculated as given in Equation (21) [15]:

$$COE = \frac{TAC}{L_{prim,AC} + L_{prim,DC}} \quad (21)$$

where  $L_{prim,AC}$  and  $L_{prim,DC}$  are the AC primary load and the DC primary load, respectively.

Among the above-presented cost parameters, NPC and COE are given higher priority during the techno-economic modeling of the proposed HREM. In addition, the environmental assessment of the proposed HREM is done considering the emission parameters that include carbon dioxide (CO<sub>2</sub>), carbon monoxide (CO), unburned hydrocarbon (UHC), particulate matter (PM), sulfur dioxide (SO<sub>2</sub>), and nitrogen oxides (NO<sub>2</sub>).

In the third step, sensitivity analysis is carried out by considering the sensitive parameters in order to achieve lower NPV and COE. The sensitive parameters include solar irradiance, wind speeds, discount rates, and diesel price. Based on these sensitive parameters, the feasible HREM configurations can be obtained, which are further analyzed and discussed to select the best configuration that satisfies the key aspects of the SDG7.

## 5. Pre-Assessment and Data Inputs for Simulation

The HREM involves a detailed assessment of the site considering the electrical load data and available renewable potential at the site location. In addition, the cost of the various components used in the HREM at the particular site is also considered. Overall, the modeling involves load assessment, resource assessment, cost assessment, and sensitive parameters.

### 5.1. Load Assessment

Electrification in India is a big challenge due to the remote and inaccessible villages, and most people live in rural areas as opposed to urban or suburban areas. At present, most villages have electrical connections in some states, but in a few other states, the electrification works are still underway. The state of Tamil Nadu, in South India, is said to be one of the fully electrified states in India. Though most villages in Tamil Nadu have access to electricity, the reliability is a major challenge. People experience long power cuts, and sometimes the occurrence of these power cuts are frequent. This has encouraged people in remote area to form a community for the development of HREMs. In the current study, a case study was undertaken based on one such remote community located in Perundurai, Tamil Nadu, India. It is geographically located at a latitude of 11.2758° N, and a longitude of 77.5830° E. The case study of the HREM was designed to fulfill the electricity needs of a remote household community. The load profile of the community on a given day is shown in Figure 6. It is observed that the community load demand patterns vary with time; for example, from 00:00–01:00 to 04:00–05:00 h, the connected load is 2 kW, then, the load profile is slightly increased to 8 kW (from 05:00–06:00 to 08:00–09:00 h), then, it maintained at a constant value of 8 kW until 16:00 h. While in the evening hours, the load increases to 12 kW (from 16:00–17:00 to 18:00–19:00 h). The demanded load peaks, i.e., 12 kW until 22:00 h and then falls to a value of 5 kW between 23:00–24:00 h. The maximum load demand, i.e., 12 kW, is observed in the evening hours around 18:00–22:00 h.

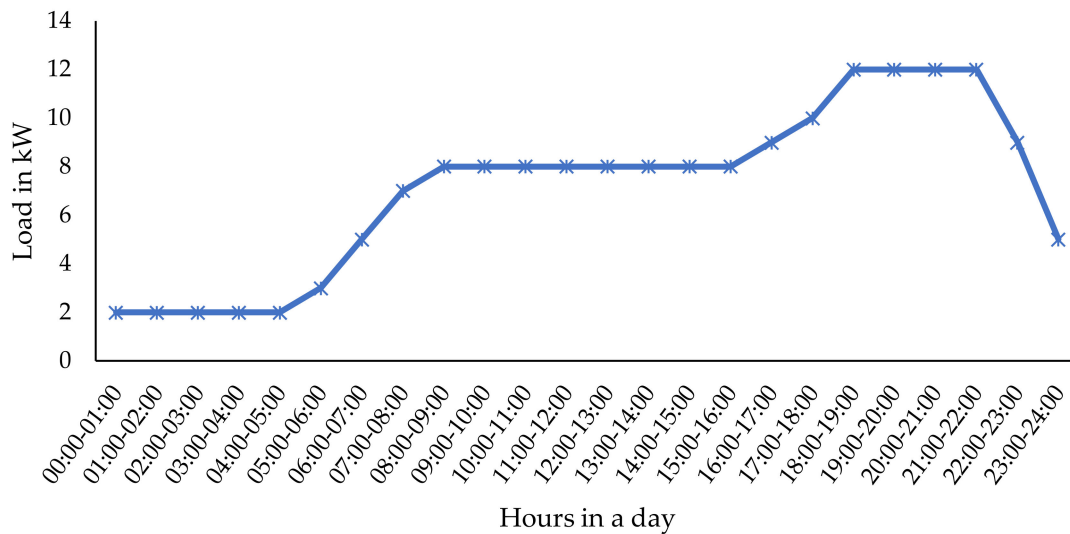


**Figure 6.** Hourly load profile of the community on a given day.

The hourly load profile for the whole year is shown in Figure S2, which shows the peak load of 20.46 kW in January. The load demand values were further analyzed to understand the seasonal patterns, and variations in the load profile are shown in Figure 7. Seasonal variations were observed and considered in the HREM modeling to ensure that the proposed system can meet the load demands considering this variation.

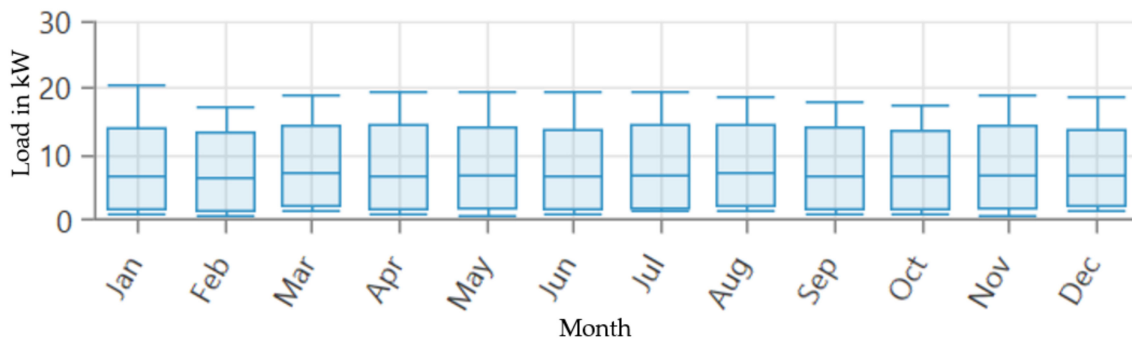


**Figure 7.** Seasonal variations in the load profile of the community for each month.

From Figure 7, it is observed that January had the peak load, and the minimum load was in February, followed by October. Hence, designing an HREM for peak loads was advisable. The observed peak load is 20.46 kW, whereas the average load is 6.89 kW. It is also observed that daily energy demand is approximately 165.44 kWh/day.

## 5.2. Resource Assessment

The two RERs used in this simulation were solar and wind energy. In the studied community, solar radiation is available nearly all year, with sunny days relatively longer in summer and slightly shorter in winter. The ambient temperature in the summer reached up to 27.98 °C at the selected site. The observed minimum ambient temperature was 22.78 °C. The solar radiation data for the chosen site was collected from the ground meteorology and solar energy database of the National Aeronautics and Space Administration (NASA). For the area under study, the average annual solar radiation was 5.12 kWh/m<sup>2</sup>/day, with a clearness index of 0.52. On a monthly basis, the solar radiation was observed to vary between 4.22 to 6.5 kWh/m<sup>2</sup>/day. The monthly variability of daily solar radiation and the clearness observed in the community are shown in Figure 8, which confirms the good solar

capacity of the selected PV system site. The hourly profile and DMap for the solar radiation are shown in Figures S3 and S4, respectively.

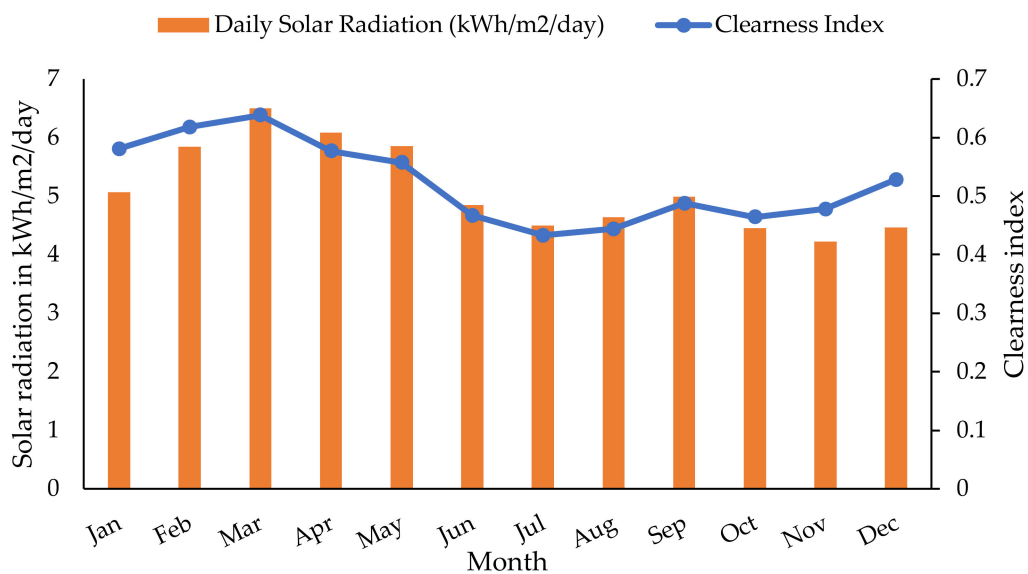


Figure 8. Daily solar radiation and clearness index.

The average monthly wind speed for study location for the last ten years was also obtained from NASA, which is 50 meters above the sea level. The wind speed ranged from 2.2 m/s to 3.45 m/s, with an average of 2.75 m/s, as shown in Figure 9. The hourly profile and DMap for the wind speeds are shown in Figures S5 and S6, respectively.

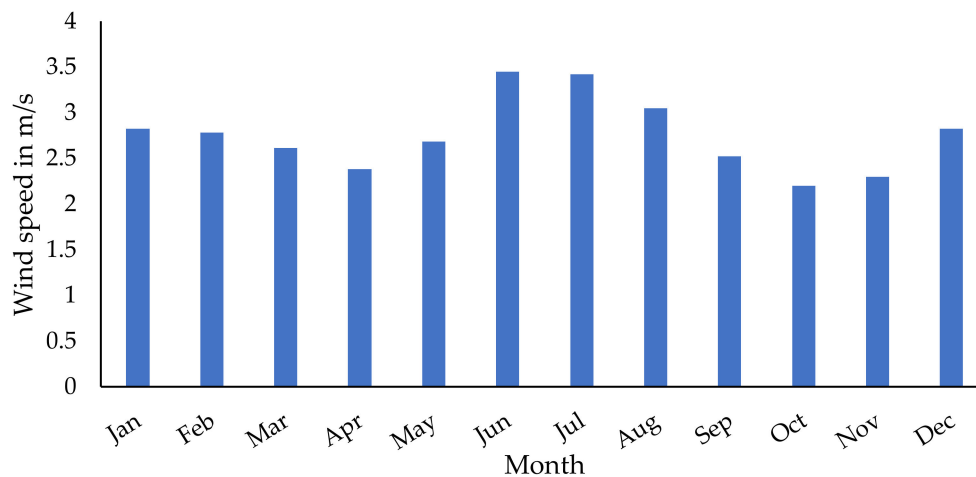


Figure 9. Monthly average wind speeds.

### 5.3. Load Following Dispatch Strategy

In the modeled HREM, there are different power generating and storage systems. Both renewable and fossil fuel-based power generators are considered. While in the operational mode, these components have to be controlled effectively, and it can be done using the dispatch strategies. In general, a dispatch strategy has a set of defined rules which are used to control and operate the power generator and storage systems in the HREM. The primary condition is to meet the load demands of the studied community even when there is a limited energy output from a renewable power generator. In this study, during the optimization of the HREM configuration, a load following (LF) dispatch strategy is used, which ensures the load demand is always met. In this strategy, when the energy output from the

renewable power generators (in this study, PV and WT) is less than load demand by the community, then LF helps to estimate the deficit loads and allows them to meet the demands by taking energy from the BESS. Whenever both the renewable energy output and BESS storage capacity are less than the required load demands, then LF helps to control the DG operation to meet the deficit energy demands by the community. During this time, the energy generated by the renewable power generators is stored in BESS for further use in the future [65].

#### 5.4. HREM Model

The proposed HREM shown in Figure 10, is planned to operate in grid-independent mode, and it has four major components: PV array, WT, DG, and BESS. Along with these components, power converters and an HREM controller were also considered. The modeled HREM in the HOMER simulation tool is shown in Figure 10a. The optimized configuration within the context of the SDG7 is shown in Figure 10b. With reference to Figure 10a, a DC bus is connected to the WT, PV array, and BESS, and a DC/AC converter is connected to the AC bus with DG.

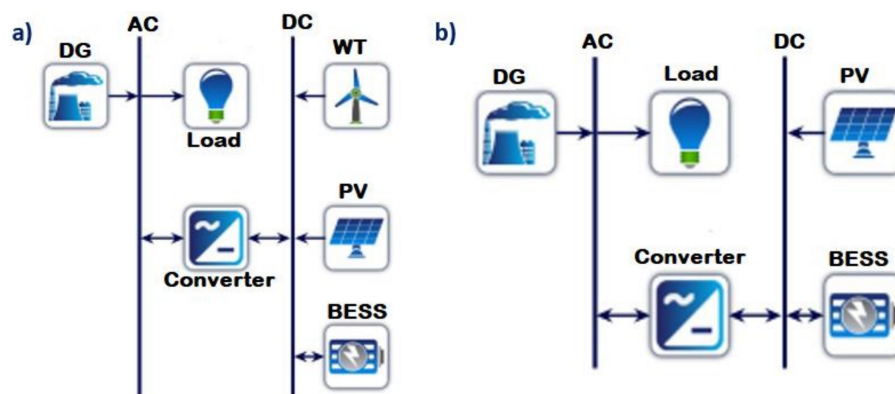


**Figure 10.** (a) Modeled HREM; (b) Optimized configuration of HREM within the context of the SDG7. [Note: DG-Diesel generator; WT-Wind turbine; PV-Photovoltaics; BESS-Battery energy storage system]

Table S1 shows the summary of the technical details of the components and other required parameters that have been given as the inputs to the HOMER hybrid model. In addition, approximate capital costs, operating and maintenance costs (O&M), and replacement costs for the capacity of the components is also provided. The cost were estimated based on the current prices in the market.

In addition to the technical and cost data, a few sensitive parameters were considered while optimizing the HREM configuration. These sensitive parameters include the nominal discount rates (%), diesel fuel price (\$/L), scaled average solar radiation ( $\text{kWh}/\text{m}^2/\text{day}$ ), and scaled average wind speed (m/s). The nominal discount rates were considered to vary between 5%–15%, diesel fuel price in India from 0.75–1.2 \$/L. Weather-related data average solar radiation and wind speeds are considered to vary between 5–7  $\text{kWh}/\text{m}^2/\text{day}$  and 2–4 m/s, respectively.

## 6. Results and Discussion

As per the enabled search space for the optimization, sensitive variables, and economic and technical constraints, the optimization was carried for the modeled the HREM configuration based on the selected components, see Figure 10. While in the optimization process, many configurations (the combination of various components to form of microgrid) were checked, and only a few combinations were selected, and the rest were omitted. Overall, 132 sensitive cases were found to be feasible, and among them, three sensitive cases were found to be suitable in the initial assessment as they had the lowest NPV and COE. However, among the three, two solutions demanded slightly higher solar radiation and wind potentials, which is not always possible in that location. In addition, the lowest value for the diesel price was considered in these three cases. At present, in India, the price of diesel fuel



is increasing, and studies also confirm that the diesel price might even go higher. Hence, we selected only one sensitive case where the NPV and COE were \$440,039 and \$0.416, respectively. This sensitive case also had three other solutions whose NPV and COE were slightly higher in terms of the renewable energy fraction, and they seemed to satisfy the SDG7 criteria. Hence, discussing those results in detail seems to be essential to conclude the HREM configuration that is suitable within the context of the SDG7. Overall, four optimized, feasible solutions of the selected sensitive case were considered. In HOMER, these were displayed as per the ascending order of the total net present cost. Then, the investigated four HREM configurations were compared to select the most cost-effective solution based on technical parameters, economic indicators, and environmental indicators or emission parameters within the context of the SDG7.

### 6.1. Technical Analysis

In Table 3, the comparison of the four optimized HREM configurations is shown. Technical analysis of the HREM provides the optimized system architecture, energy production and consumption, and renewable fraction. In all the obtained feasible solutions, the battery was included, which allows a storage facility for excess energy. Depending upon the configuration, the sizing of the battery varied. Also, the sizes of the other components like PV, WT, and DG were varied. The sizes of the components were optimized by minimizing cost. Among the obtained four configurations, the HREM was able to meet 100% energy demand only in two cases (i.e., PV + DG + BESS and PV + WT + DG + BESS). In the other two configurations (PV + BESS and PV + WT + BESS), the HREM had unmet electricity load, which was <40 kWh/y, but the system generated excess electricity, which is not economically viable to store, as the BESS capacity addition would increase the financial burdens on the community.

**Table 3.** Comparison of selected technical parameters for the feasible hybrid renewable energy microgrid (HREM) configurations.

Parameters	PV + DG + BESS	PV + WT + DG + BESS	PV + BESS	PV + WT + BESS
HREM system architecture	PV—40.3 kW DG—23 kW BESS—181 strings	PV—40.3 kW WT—3 kW (1) DG—23 kW BESS—186 strings	PV—133 kW BESS—324 strings	PV—133 kW WT—3 kW (1) BESS—327 strings
Energy production	PV—75,317 kWh/y DG—12,051 kWh/y Total—87,368 kWh/y	PV—75,247 kWh/y WT—176 kWh/y DG—12,015 kWh/y Total—87,438 kWh/y	PV—247,951 kWh/y Total—247,951 kWh/y	PV—247,951 kWh/y WT—176 kWh/y Total—248,127 kWh/y
Energy consumption	Primary load—60,386 kWh/y			
Unmet electric load	0 kWh/y	0 kWh/y	37.4 kWh/y	33.8 kWh/y
Capacity shortage	0 kWh/y	0 kWh/y	59.8 kWh/y	55.8 kWh/y
Excess energy	18,868 kWh/y	18,976 kWh/y	177,148 kWh/y	177,334 kWh/y
Renewable fraction	80%	80.1%	100%	100%

Note: PV-Photovoltaics; DG-Diesel generator; BESS-Battery energy storage system; WT-Wind turbine

The monthly average electric power production from the obtained optimized HREM configuration is presented in Figure 11. It is noticeable that the power produced in all the configuration was sufficient to meet the load demand. Monthly electric power production from the PV + DG + BESS and PV + WT + DG + BESS configurations were observed to maintain a similar trend throughout the year, whereas the other two configurations performed differently when compared. However, the power production from PV + BESS and PV + WT + BESS was observed to be more or less the same.

In all the four configurations, the share of PV was higher. For the PV + DG + BESS and PV + WT + DG + BESS configurations, the power production from PV was higher than that from DG and WT, resulting in a renewable fraction of ~80%. Between the used two renewables (PV and WT), energy from

PV was higher in all the configurations. It was also understood that whenever power from renewables was less, as per the LF dispatch strategy, the DG had served the load.

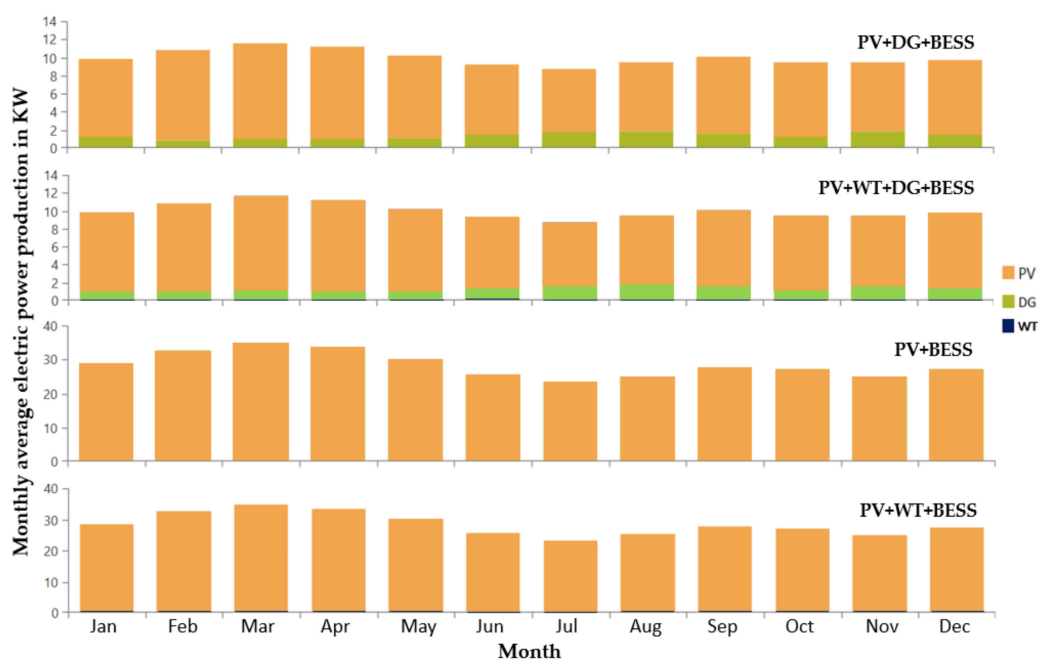


**Figure 11.** Monthly average power production in four feasible HREM configurations. [Note: PV-Photovoltaics; DG-Diesel generator; BESS-Battery energy storage system; WT-Wind turbine].

In the other two configurations (i.e., PV + BESS and PV + WT + BESS), the renewable fraction was almost close to 100%. However, in these two configurations, the storage was limited, and the excess energy was left as waste. It was observed that some percentage of energy demand was not met. In addition, the capacity shortage was also observed. As the estimated renewable fraction was close to 100% in PV + BESS and PV + WT + BESS, selecting these configurations as the most feasible ones may not be the right decision. The reason is there might be uncertainties in power supplies due to the intermittent nature of renewables. In addition, BESS capacity is also uncertain here. This uncertainty was clearly observed through the simulation study. Hence, the PV + BESS and PV + WT + BESS configurations were omitted. Based on technical analysis, the configurations PV + DG + BESS and PV + WT + DG + BESS seemed to perform well and would be suitable for the community. However, the decision to select these can be made only after the economic and environmental analysis presented in subsequent sections.

## 6.2. Economic Analysis

Four different HREM configurations were found to be feasible. These configurations, along with the considered economic indicators, are shown in Table 4. It is noticeable that the cost of electricity seems to be lower in the PV + DG + BESS configuration when compared to the other three configurations. The cost of electricity for PV + DG + BESS, PV + WT + DG + BESS, PV + BESS, and PV + WT + BESS are 0.4157 \$/kWh, 0.4382 \$/kWh, 0.6319 \$/kWh, and 0.6555 \$/kWh, respectively. The net present costs, annualized costs, operating and maintenance costs, replacement costs, and fuel costs are quite low in the case of the PV + DG + BESS based HREM configuration. The initial capital cost was low for the PV + DG + BESS configuration; hence, it was affordable by the community (it is one of the recommended configurations within the context of the SDG7 based on the technical analysis). The other configuration (i.e., PV + WT + DG + BESS) had a slightly higher COE, i.e., 0.0225 \$/kWh, but the initial capital cost of this configuration was quite high, i.e., around \$19,373.01 when compared to PV + DG + BESS. Hence, based on the economic analysis of the HREM configuration, PV + DG +

BESS was recommended considering the affordable aspect of the SDG7. To understand this, the NPCs based on the components used in each HREM configuration are shown in Figure S7.

**Table 4.** Comparison of economic indicators for the feasible hybrid renewable microgrid (HREM) configurations.

Economic Indicators	PV + DG + BESS	PV + WT + DG + BESS	PV + BESS	PV + WT + BESS
Cost of electricity (\$)	0.4157	0.4382	0.6319	0.6555
Net present cost (\$)	440,038.84	463,824.70	668,370.80	693,396.90
Annualized cost (\$)	25,105.15	26,462.18	38,131.97	39,559.76
Initial capital cost (\$)	170,919.23	190,292.24	435,612.61	454,552.17
Operating and maintenance cost (\$/y)	53,575.06	57,370.08	80,067.14	83,747.99
Replacement cost (\$)	161,894.52	173,999.49	192,266.17	203,231.30
Fuel cost (\$)	77,382.17	76,803.08	0.00	0.00
Salvage cost (\$)	23,732.13	34,640.99	39,575.16	48,134.51

Note: PV-Photovoltaics; DG-Diesel generator; BESS-Battery energy storage system; WT-Wind turbine

### 6.3. Environmental Analysis

The following four HREM configurations were found to be the most feasible in this study: PV + DG + BESS; PV + WT + DG + BESS; PV + BESS; and PV + WT + BESS. In Table 5, the feasible HREM configurations were compared by considering six different emission parameters. These include CO<sub>2</sub>, CO, UHC, PM, SO<sub>2</sub>, and NO<sub>2</sub>. In HOMER optimization, emissions are generally considered only when fossil fuel-based power generation is available in the HREM configuration. Hence, these emission values are not sufficient to decide which configuration seems to be sustainable. Therefore, considering the emissions based on life cycle emissions of the other power generating systems is essential. In Table 6, emissions based on the service life of the components was estimated by considering the life cycle emissions of each component used in the four different HREM configurations. From the literature, it was identified that a crystalline PV technology based solar module emits 55 g CO<sub>2</sub>/kWh, 0.38 g SO<sub>2</sub>/kWh, and 0.2 g NO<sub>2</sub>/kWh [66].

The emissions from the WT was considered as 106 g CO<sub>2</sub>/kWh [67]. The battery was considered to emit 338 kg CO<sub>2</sub>/kWh based on its life cycle, in addition to CO<sub>2</sub>, the batteries SO<sub>2</sub> emissions were 2.23 g/kWh [68]. From Table 6, it is noticeable that CO<sub>2</sub> emissions were possible in all the configurations. PV + DG + BESS generated fewer CO<sub>2</sub> emissions, i.e., 85,104.31 kg in its service life, whereas the other configurations that include PV + WT + DG + BESS, PV + BESS, and PV + WT + BESS generated 86,661.88 kg, 1,23,149.31 kg, and 1,24,181.97 kg, respectively. After CO<sub>2</sub>, the next highest released emissions were CO, and in this study, CO emissions were found in only two configurations. The observed CO emissions from PV + DG + BESS and PV + WT + DG + BESS were 124.63 kg/y and 123.78 kg, respectively. Overall, the observed environmental emissions from the PV + DG + BESS-based HREM were substantially lower than the other three configurations. The increase in CO<sub>2</sub> emissions in these three configurations is due to diesel fuel consumption and the huge capacities of BESS. It is suggested that an HREM configuration with lower emissions seems to be sustainable. Overall, based on the emission and environmental analyses, the HREM configuration of PV + DG + BESS is recommended considering the sustainable aspect of the SDG7.

**Table 5.** Comparison of emission parameters for hybrid renewable energy microgrid (HREM) configurations based on diesel generator (DG) operation.

Emission Parameter	PV + DG + BESS	PV + WT + DG + BESS	PV + BESS	PV + WT + BESS
	Values (kg/y)			
CO <sub>2</sub>	11,556	11,470	0	0
CO	72.8	72.3	0	0
UHC	3.18	3.15	0	0
PM	0.441	0.438	0	0
SO <sub>2</sub>	28.3	28.1	0	0
NO <sub>2</sub>	68.4	67.9	0	0

Note: PV-Photovoltaics; DG-Diesel generator; BESS-Battery energy storage system; WT-Wind turbine

**Table 6.** Comparison of emission parameters for hybrid renewable energy microgrid (HREM) configurations considering the life cycle emissions of all the components.

Emission Parameter	PV + DG + BESS	PV + WT + DG + BESS	PV + BESS	PV + WT + BESS
	Values (kg/Service Life)			
CO <sub>2</sub>	85,104.31	86,661.88	1,23,149.31	1,24,181.97
CO	124.63 *	123.78 *	NA	NA
UHC	5.44 *	5.39 *	NA	NA
PM	0.75 *	0.75 *	NA	NA
SO <sub>2</sub>	77.47 <sup>a</sup>	77.12 <sup>a</sup>	94.95 <sup>a</sup>	94.95 <sup>a</sup>
NO <sub>2</sub>	132.16 <sup>b</sup>	131.29 <sup>b</sup>	49.59 <sup>b</sup>	49.59 <sup>b</sup>

Note: NA—not accounted; DG—Diesel generator; \* accounted without considering the renewables; <sup>a</sup> accounted considering photovoltaics (PV), wind turbine (WT), and battery energy storage system (BESS); <sup>b</sup> accounted considering only PV.

#### 6.4. Performance of PV + DG + BESS HREM Configuration

Here, the performance of the PV + DG + BESS in terms of techno-economic-environmental analysis is discussed. The modeled HREM primary objective of meeting its load demand was served. From Figure S8, it is observed that the AC primary load of the community was clearly served by the HREM with the PV + DG + BESS configuration. Figure 12 represents the performance of the PV array considering the incident solar on it and the power outputs produced. It is understood that the PV array of 40.3 kW received a sufficient amount of solar power potential. In some situations, the incident solar radiations were much lower. However, on average, the incident solar power potential varied between 0.2 and 1.3 kW/m<sup>2</sup> per hour. Accordingly, the output power from the PV array was produced, which then served as the primary load of the community. To quantify the exact PV power production hours, DMap was plotted and is shown in Figure S9.

The DMap shows that PV power production was mostly between 06:30 and 18:00 in a day. It was also observed that the PV array had a average output per hour and day of 8.6 kW and 206 kW, respectively. The PV array was operated with a capacity factor of 21.3%. The total operating hours of the PV array were 4387 h/y, and its total energy production was 75,317 kWh/y Overall, the PV penetration was observed as 125%, and the levelized cost of electricity for PV alone was observed as 0.0817 \$/kWh.

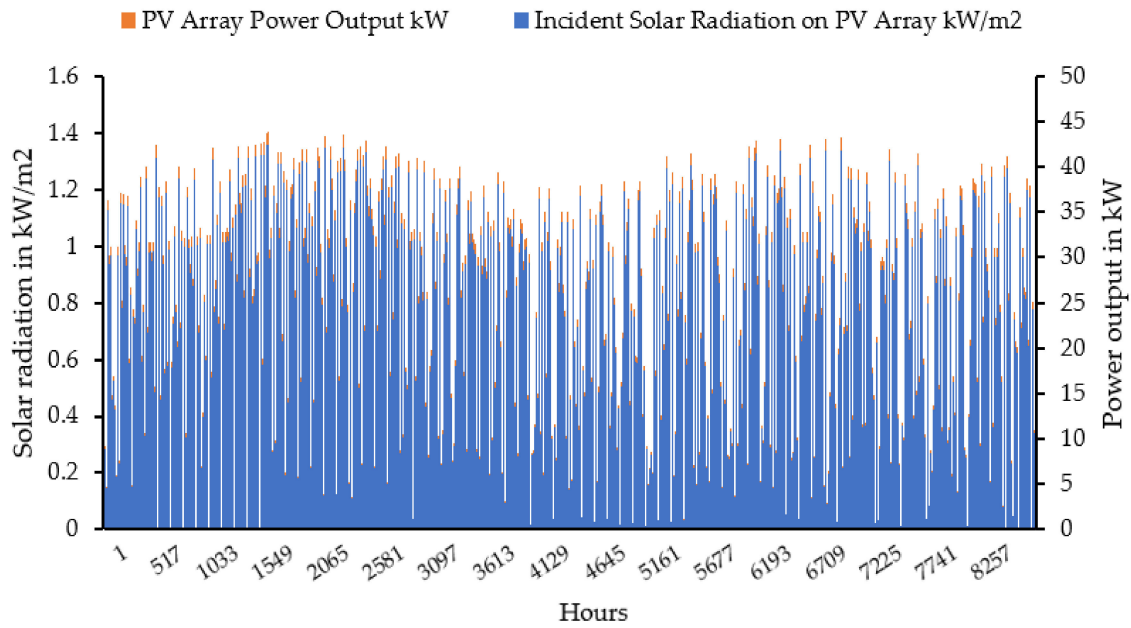


**Figure 12.** Power output from the PV array in the photovoltaic (PV) + DG + battery energy storage system (BESS) configuration of the HREM.

In the PV + DG + BESS HREM configuration, only PV is a renewable power generator. The daily profile of renewables-based power potential is shown in Figure 13 for each month. It is evident that renewable power outputs were only available during the daytime (around 11–12 h from the PV array). The rest of the hours, the load was met either by BESS or DG. However, as per the LF dispatch strategy, at each point of time, the load was compared, and new deficit energies were estimated by controlling the HREM power generators and storage systems effectively. Whenever renewable power and the stored energy were less than in BESS, the LF strategy controlled the DG to serve as the primary load, and during this time, any amount of power generated by the renewables was fed to BESS.

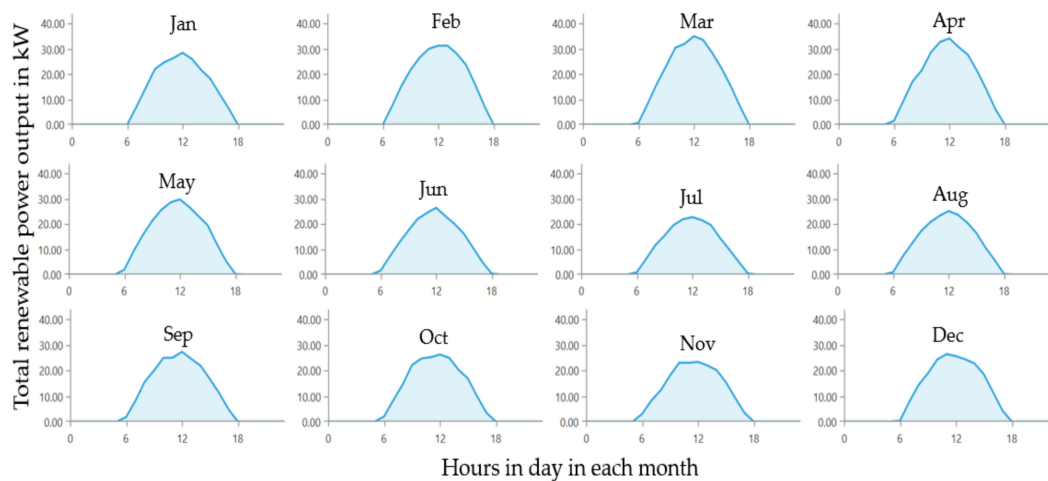


**Figure 13.** Total renewable power produced in the HREM configuration of PV + DG + BESS.

To understand the load meeting requirements, we plotted a graph for total renewable power outputs and load served, see Figure 14. From Figure 14, it is observed that in a few hours, excess energy was generated, which can be stored in BESS. In addition, it is noticeable that the PV power varied and could not meet the load demands at particular times, and during these conditions, either BESS or the DG was operated.

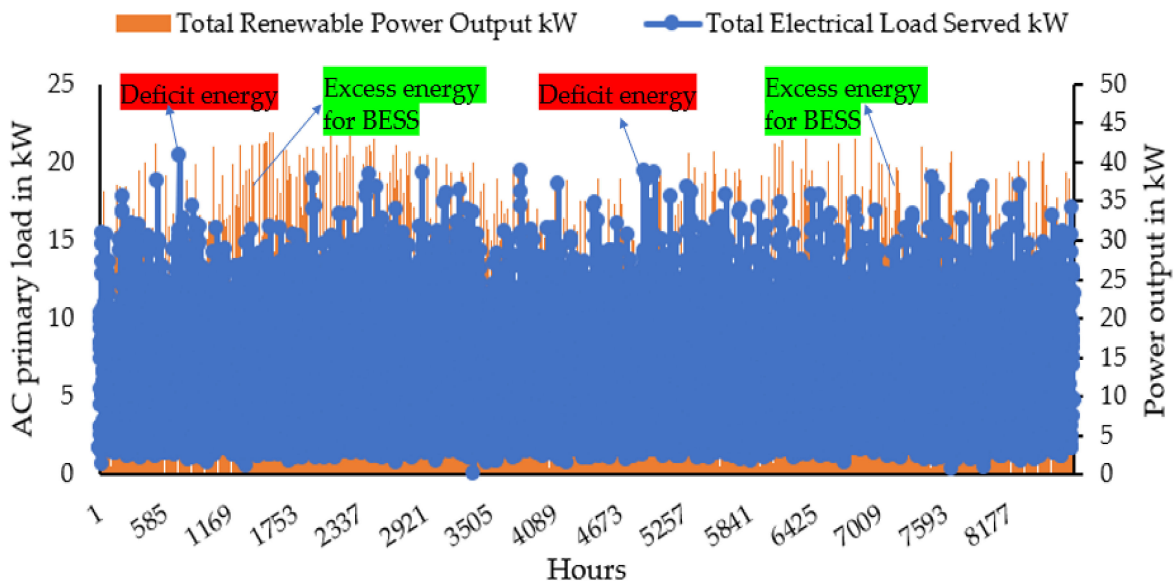


**Figure 14.** Alternating current (AC) primary load and total renewable power output in the PV + DG + BESS HREM configuration.

The BESS performance characteristics are presented in Figure 15. Here, the maximum charge power was observed to vary between 0.47 kW and 47.48 kW at any given time. Similarly, the maximum discharge power range was 0.199 kW to 47.26 kW. The state of the charge characteristics of the BESS is shown in Figure 16.

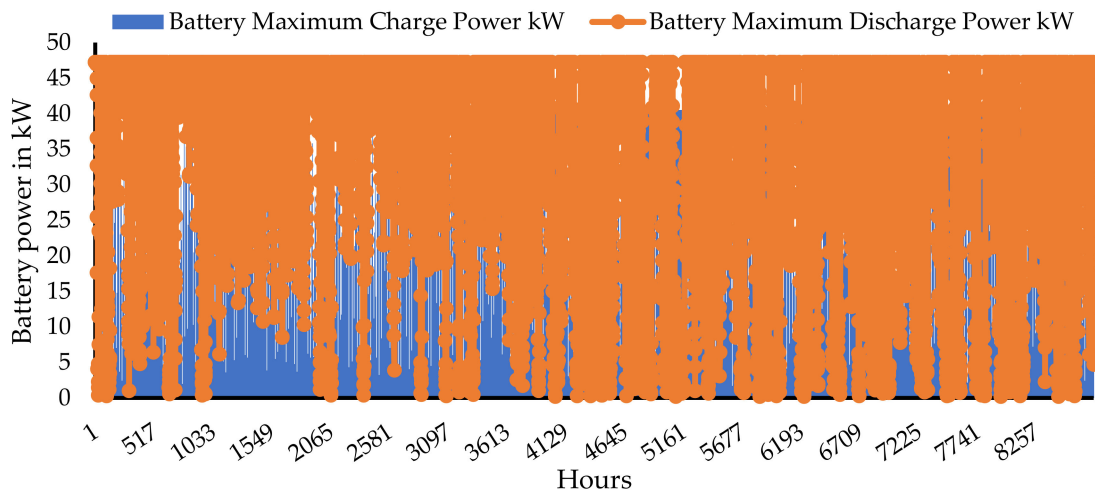


**Figure 15.** BESS charge and discharge power in the PV + DG + BESS HREM configuration.

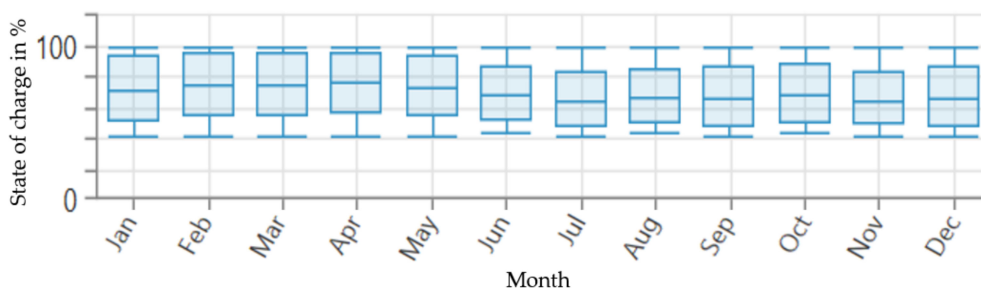


**Figure 16.** State of the charge of the BESS in the PV + DG + BESS HREM configuration.

The excess energy produced from the HREM was observed to be around 21.6% (18,868 kWh/y) of the total production, which was then stored in the BESS. The optimized BESS was based on 181 strings; each string had one battery (total equivalent to 181 kWh). The considered battery autonomy was 15.8 h. The nominal storage capacity was 181 kWh, but the usable capacity was only 109 kWh. The battery lifetime throughput was observed as 144,800 kWh with an expected life of 5.78 years. On an annual basis, the amount of energy input to the battery was around 27,913 kWh/y. The battery delivered an output of 22,422 kWh/y, and the leftover 5593 kWh/y was dissipated to the outer environment as thermal losses. Apart from this, a storage depletion of 103 kWh/y was observed. The continuous operation of the battery causes it to wear out, which is generally influenced by the overall energy storage and its associated costs. This wear out is generally represented in terms of cost, and in this case, a storage wear cost of 0.419 \$/kWh was observed.

From Figure 14, it is noticed that at some points the renewable power as well as the BESS fail to meet the energy demand. During these times, the LF strategy allows the DG to come into operation to serve as the primary energy provider. DG is also one of the components that generates power in the optimized HREM configuration, and the power produced and the diesel consumed by the DG are shown in Figure 17. The mean, minimum, and maximum electrical outputs from the DG were 9.86 kW, 5.75 kW, and 20.5 kW, respectively. The operating hours of the DG were illustrated in DMap and are shown in Figure S10. The operational characteristics of the DG were also considered, including hours of operation (i.e., 1222 h/y), number of starts (638 starts/y), operational life (i.e., 12.3 y), and capacity factor (i.e., 5.98%). The marginal generation cost was 0.236 \$/kWh.

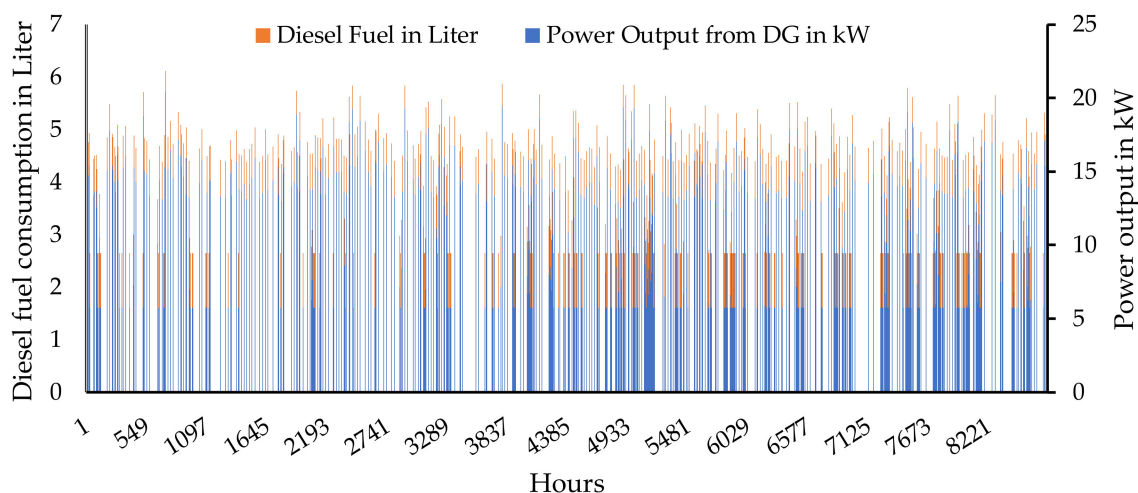


**Figure 17.** Diesel consumption and power outputs from the DG in the HREM configuration of PV + DG + BESS.

The daily profile of diesel fuel consumption is shown in Figure S11 for each month. It is observed that approximately 4,415 L of fuel was consumed. The specific fuel consumption was 0.366 L/kWh. The fuel energy input was 43,442 kWh/y, whereas the electrical output from the DG was 12,051 kWh/y, and finally, the average electrical efficiency was 27.7%.

Economic analysis of the optimized HREM configuration, i.e., PV + DG + BESS, was understood by considering the cash flow in the lifetime of the HREM configuration. In Figure 18, the cash flow by cost type and component type are presented. Throughout the life of an HREM, the replacement cost occurred in the 6th year (i.e., \$54,300), 12th year (i.e., \$54,300), 13th year (i.e., \$11,500), 15th year (i.e., \$4271.61), and 18th year (i.e., \$54,300). BESS and DG are the components that would have to be replaced, and in the 15th year, the converter would also be replaced. The operational costs were also considered. The observed net present cost and cost of electricity for this optimized configuration were \$440,038.80 and \$0.4157, respectively. This seems to be an affordable case and can meet the affordable electricity criteria of the SDG7.

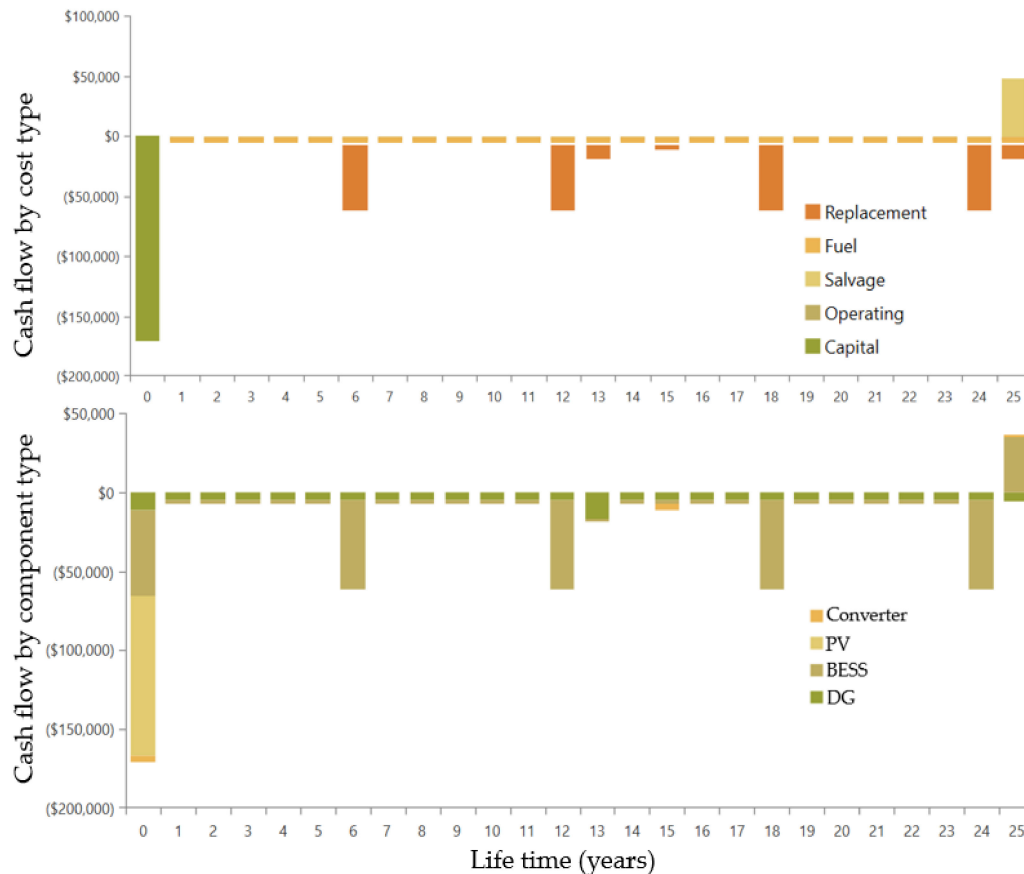


**Figure 18.** Cash flows in the optimized HREM (PV + DG + BESS) configuration by cost and component type.

The environmental analysis was based on the amount of emissions released from the PV + DG + BESS based HREM configuration. From the obtained configuration, the value of released emissions based on DG operation included CO<sub>2</sub>, CO, UHC, SO<sub>2</sub>, and NO that were 11,556 kg/y, 72.8 kg/y, 3.18 kg/y, 0.441 kg/y, 28.3 kg/y, and 68.4 kg/y, respectively. However, accounting for these emissions alone may not be sufficient; hence, the life cycle emissions of all the components were considered. Overall, PV + DG + BESS generated fewer CO<sub>2</sub> emissions, i.e., 85,104.31 kg in its service life, whereas the other configurations that included PV + WT + DG + BESS, PV + BESS, and PV + WT + BESS generated 86,661.88 kg, 1,23,149.31 kg, and 1,24,181.97 kg, respectively.

Overall, the technical-economic and environmental analysis of the PV + DG + BESS configuration suggests that the HREM operates effectively to deliver the required energy demands of the residential community.



### 6.5. HREM Configurations within the Context of the SDG7

As per the SDG7, the configuration should be affordable, reliable, sustainable, and modern, ensuring energy access to all. In our study, we considered a residential community load, and among the studied configurations, whichever configurations had zero unmet electricity demands, then those HREM configurations would provide energy access to all in the community. In addition, we also found that the discussion related to the HREM configuration in relation to the SDG7 key aspects is essential for identifying the best solution. For mapping, we used a few indicators; based on those indicators, the optimization of this proposed HREM was done. Under the SDG7, the indicators for assessing the affordable aspect are lower COE, lower NPV, and lower capital investments; reliable are continuous power supply, minimize the energy shortage, and quality of power is ensured (the configuration that has DG and BESS with enough backup power can also meet these criteria, in addition, the DG can serve the load whenever the energy from renewables and BESS is low, and it is controlled based on LF dispatch strategy). In a similar manner, the indicators for assessing sustainability are higher renewable fraction and minimum emissions. The last criteria for the HREM is that it should be a modern power generating system, and we believe the proposed MGs; hybrid power systems; and community MGs directly fall under the category of modern power systems. In addition, these MGs can be capable of operating with additional features such as energy trading with other community MGs. Based on this, all the considered indicators seem to be favorable for PV + DG + BESS. The obtained four HREM configurations are mapped within the context of the SDG7 in Table 7.

**Table 7.** Mapping of the optimized hybrid renewable energy microgrid (HREM) configuration indicators within the context of the sustainable development goal (SDG7).

Criteria and Aim	SDG7 Criteria	Indicator with Units	HREM Configuration			
			PV + DG + BESS	PV + WT + DG + BESS	PV + BESS	PV + WT + BESS
Criteria	Affordable	Lower NPC (\$)	440,038.84	463,824.70	668,370.80	693,396.90
		Lower COE (\$/kWh)	0.4157	0.4382	0.6319	0.6555
		Lower initial capital cost (\$)	170,919.23	190,292.24	435,612.61	454,552.17
	Reliable	Continuous power supply (when renewables and BESS fail)	DG helps continuous power supply	DG and BESS helps with continuous power supply	Only BESS has to support the continuous power supply, but if we increase capacity it will add a financial burden to the community	
		Excess electricity or buffer for future (kWh/y)	18,868	18,976	177,148	177,334
		Minimize the capacity shortage (kWh/y)	0	0	59.8	55.8
		Quality of power *	Optimized results suggest the quality of power is ensured in each HREM configuration.			
	Sustainable	Lower emissions per year (kg/y) <sup>a</sup>	11,556	11,470	0	0
		Lower emissions per service life (kg/service life) <sup>b</sup>	85,104.31	86,661.88	1,23,149.31	1,24,181.97
		Higher renewable energy fraction (%)	80	80.1	100	100
	Modern	MGs <sup>b</sup>	✓	✓	x	✓
		Hybrid power systems <sup>b</sup>	✓	✓	x	✓
		Community MGs <sup>b</sup>	✓	✓	x	✓
	Aim	Energy access	Unmet electricity (kWh/y)	0	0	37.4

Note-1: \* indicates that quality of power is ensured for all the HREM configurations, however, considering this indicator as a research objective and modeling in terms of electrical aspects would give more interesting results; <sup>a</sup> indicates the CO<sub>2</sub> emissions based on the service life of the system components used in HREM considering their life cycle emissions; <sup>b</sup> indicates that any system having two or more power generators and serving a community load is considered as a hybrid power system (either renewable-based or non-renewable based) and MGs. Note-2: PV-Photovoltaics; DG-Diesel generator; WT-Wind turbine; BESS-Battery energy storage system

## 7. Conclusions

In this work, a grid-independent HREM was developed to satisfy the electricity demand of a remote community in South India. The analysis was carried out in the HOMER software tool, and a cost-effective configuration of the HREM was attained. Simulations were carried out based on load profiles and available RERs in the study location. From the simulation analyses, it is evident that considering component sizes, cash flow summary, electrical energy production, and greenhouse gas emissions, the HREM system comprising PV/DG/BESS was found to be the most feasible. The following conclusions were derived based on the techno-economic-environmental analysis.

- A high renewable fraction was ensured, and in addition, the load demand was met continuously.
- Surplus energy from the generation sources was stored in the battery, and that can be used in emergency or deficit situations.
- The proposed LF dispatch strategy ensured effective operation and met the set goals.
- Lower net present cost and cost of electricity were ensured, and this would make the HREM affordable for the community households.
- The obtained HREM configuration was found to be sustainable from the environmental perspective as it produced lower emissions than the other configurations.
- Overall, the proposed HREM configuration was identified to be within the context of the SDG7.

**Supplementary Materials:** The following are available online at <http://www.mdpi.com/2071-1050/12/10/3944/s1>, Figure S1: The power curve of a wind turbine representing wind turbine performance characteristics, Figure S2. Hourly load profile of the community for the whole year, Figure S3. Hourly solar radiation potential for the whole year, Figure S4. DMap showing the solar radiation potential in hours, Figure S5. Hourly wind speeds available for whole year, Figure S6. DMap showing the wind potential in hours, Figure S7. The net present cost of the four feasible HREM configurations, Figure S8. Primary load and primary load served patterns by the PV + DG + BESS HREM configuration, Figure S9. DMap showing the solar PV power production hours in the PV + DG + BESS HEEM configuration, Figure S10. DMap showing the power production hours from the diesel generator, Figure S11. Diesel fuel consumption in the PV + DG + BESS based HREM configuration, Table S1: Technical and cost details of the components used in designing the HREM.

**Author Contributions:** Conceptualization, N.M.K. and S.S.C.; Data curation, N.M.K.; Formal analysis, N.M.K.; Funding acquisition (towards APC), G.M.S.; Methodology, N.M.K. and S.S.C.; Resources, S.S.C.; Software, N.M.K. and S.S.C.; Supervision, S.S.C.; Visualization, N.M.K.; Writing—original draft preparation, N.M.K. and A.A.C.; Writing—review and editing, N.M.K., S.S.C., R.M.E., and G.M.S. All authors have read and agreed to the published version of the manuscript.

**Conflicts of Interest:** The authors declare no conflict of interest.

## References

1. Sustainable Development Goal 7 (SDG). Available online: <https://sustainabledevelopment.un.org/sdg7> (accessed on 16 February 2020).
2. Ajadi, T.; Boyle, R.; Strahan, D.; Kimmel, M.; Collins, B.; Cheung, A.; Becker, L. *Global Trends in Renewable Energy Investment 2019*; Frankfurt School-UNEP Centre/BNEF: Frankfurt, Germany, 2019; Available online: <http://www.fs-unep-centre.org> (accessed on 16 February 2020).
3. Power Sector at a Glance ALL INDIA, Govt. of India. Available online: <https://powermin.nic.in/en/content/power-sector-glance-all-india> (accessed on 16 February 2020).
4. Singh, R.K. India's Renewable Energy Capacity Crosses 80GW-Mark. Available online: <https://economictimes.indiatimes.com/industry/energy/power/indias-renewable-energy-capacity-crosses-80gw-mark-r-k-singh> (accessed on 16 February 2020).
5. Kumar, A.; Kumar, N.; Baredar, P.; Shukla, A. A review on biomass energy resources, potential, conversion and policy in India. *Renew. Sustain. Energy Rev.* **2015**, *45*, 530–539. [CrossRef]
6. Sachs, J.; Schmidt-Traub, G.; Kroll, C.; Lafortune, G.; Fuller, G. *Sustainable Development Report 2019*; Bertelsmann Stiftung and Sustainable Development Solutions Network (SDSN): New York, NY, USA, 2019.
7. BP Magazine. Available online: <https://www.bp.com/en/global/corporate/energy-economics/statistical-review-ofworldenergy/renewable-energy.html> (accessed on 27 November 2019).

8. Sharma, A.; Chaturvedi, S.; Choudhury, S. India's Power Network Breaks Down. *The Wall Street Journal*. 31 July 2012. Available online: <https://www.wsj.com/articles/SB10000872396390444405804577560413178678898> (accessed on 16 February 2020).
9. Zsiborács, H.; Baranyai, N.H.; Vincze, A.; Zentkó, L.; Birkner, Z.; Máté, K.; Pintér, G. Intermittent renewable energy sources: The role of energy storage in the European power system of 2040. *Electronics* **2019**, *8*, 729. [[CrossRef](#)]
10. Chand, A.A.; Prasad, K.A.; Mamun, K.A.; Sharma, K.R.; Chand, K.K. Adoption of Grid-Tie Solar System at Residential Scale. *Clean. Technol.* **2019**, *1*, 224–231. [[CrossRef](#)]
11. Lopes, J.P.; Hatziargyriou, N.; Mutale, J.; Djapic, P.; Jenkins, N. Integrating distributed generation into electric power systems: A review of drivers, challenges and opportunities. *Electr. Power Syst. Res.* **2007**, *77*, 1189–1203. [[CrossRef](#)]
12. Islam, F.R.; Mamun, K.A. Possibilities and challenges of implementing renewable energy in the light of PESTLE & SWOT analyses for island countries. In *Smart Energy Grid Design for Island Countries*; Springer: Cham, Switzerland, 2017; pp. 1–19.
13. Karthik, N.; Parvathy, A.K.; Arul, R. Optimal Operation of Microgrids-A Survey. *Int. J. Appl. Power Eng.* **2018**, *7*, 179–185.
14. Islam, F.R.; Prakash, K.; Mamun, K.A.; Lallu, A.; Pota, H.R. Aromatic network: A novel structure for power distribution system. *IEEE Access* **2017**, *5*, 25236–25257. [[CrossRef](#)]
15. Ferraro, M.; Brunaccini, G.; Sergi, F.; Aloisio, D.; Randazzo, N.; Antonucci, V. From Uninterruptible Power Supply to resilient smart micro grid: The case of a battery storage at telecommunication station. *J. Energy Storage* **2020**, *28*. [[CrossRef](#)]
16. Sawle, Y.; Gupta, S.C.; Bohre, A.K. Review of hybrid renewable energy systems with comparative analysis of off-grid hybrid system. *Renew. Sustain. Energy Rev.* **2018**, *81*, 2217–2235. [[CrossRef](#)]
17. Vishnupriyan, J.; Manoharan, P.S. Optimizing an on-grid hybrid power system in educational institution in Tamil Nadu, India. In *Green Buildings and Sustainable Engineering*; Springer: Singapore, 2018; pp. 93–103.
18. Amrollahi, M.H.; Bathaee, S.M.T. Techno-economic optimization of hybrid photovoltaic/wind generation together with energy storage system in a stand-alone micro-grid subjected to demand response. *Appl. Energy* **2017**, *202*, 66–77. [[CrossRef](#)]
19. Shafiullah, G.M.; Amanullah, M.T.O.; Ali, A.S.; Jarvis, D.; Wolfs, P. Prospects of renewable energy—A feasibility study in the Australian context. *Renew. Energy* **2012**, *39*, 183–197. [[CrossRef](#)]
20. Shoeb, M.; Shafiullah, G.M. Renewable energy integrated islanded microgrid for sustainable irrigation—A Bangladesh perspective. *Energies* **2018**, *11*, 1283. [[CrossRef](#)]
21. Akhtari, M.R.; Baneshi, M. Techno-economic assessment and optimization of a hybrid renewable co-supply of electricity, heat and hydrogen system to enhance performance by recovering excess electricity for a large energy consumer. *Energy Convers. Manag.* **2019**, *188*, 131–141. [[CrossRef](#)]
22. Ali, I.; Shafiullah, G.M.; Urmee, T. A preliminary feasibility of roof-mounted solar PV systems in the Maldives. *Renew. Sustain. Energy Rev.* **2018**, *18*, 18–32. [[CrossRef](#)]
23. Brka, A.; Al-Abdeli, Y.M.; Kothapalli, G. The interplay between renewables penetration, costing and emissions in the sizing of stand-alone hydrogen systems. *Int. J. Hydrog. Energy* **2015**, *40*, 125–135. [[CrossRef](#)]
24. Baek, S.; Park, E.; Kim, M.G.; Kwon, S.J.; Kim, K.J.; Ohm, J.Y.; del Pobil, A.P. Optimal renewable power generation systems for Busan metropolitan city in South Korea. *Renew. Energy* **2016**, *88*, 517–525. [[CrossRef](#)]
25. Panayiotou, G.; Kalogirou, S.; Tassou, S. Design and simulation of a PV and a PV Wind standalone energy system to power a household application. *Renew. Energy* **2012**, *37*, 355–363. [[CrossRef](#)]
26. Gangwar, S.; Bhanja, D.; Biswas, A. Cost, reliability, and sensitivity of a stand-alone hybrid renewable energy system—A case study on a lecture building with low load factor. *J. Renew. Sustain. Energy* **2015**, *7*, 013109. [[CrossRef](#)]
27. Islam, A.K.M.S.; Rahman, M.M.; Mondal, M.A.H.; Alam, F. Hybrid energy system for St. Martin Island, Bangladesh: An optimized model. *Procedia Eng.* **2012**, *49*, 179–188. [[CrossRef](#)]
28. Colantoni, A.; Allegrini, E.; Boubaker, K.; Longo, L.; Di Giacinto, S.; Biondi, P. New insights for renewable energy hybrid photovoltaic/wind installations in Tunisia through a mathematical model. *Energy Convers. Manag.* **2013**, *75*, 398–401. [[CrossRef](#)]

29. Ahmad, J.; Imran, M.; Khalid, A.; Iqbal, W.; Ashraf, S.R.; Adnan, M.; Ali, S.F.; Khokhar, K.S. Techno economic analysis of a wind-photovoltaic-biomass hybrid renewable energy system for rural electrification: A case study of Kallar Kahar. *Energy* **2018**, *148*, 208–234. [[CrossRef](#)]
30. Baghdadi, F.; Mohammedi, K.; Diaf, S.; Behar, O. Feasibility study and energy conversion analysis of stand-alone hybrid renewable energy system. *Energy Convers. Manag.* **2015**, *105*, 471–479. [[CrossRef](#)]
31. Enevoldsen, P.; Sovacool, B.K. Integrating power systems for remote island energy supply: Lessons from Mykines, Faroe Islands. *Renew. Energy* **2016**, *85*, 642–648. [[CrossRef](#)]
32. Sharafi, M.; ELMekkawy, T.Y. Multi-objective optimal design of hybrid renewable energy systems using PSO-simulation based approach. *Renew. Energy* **2014**, *68*, 67–79.
33. Biswas, A.; Kumar, A. Techno-economic optimization of a stand-alone PV/PHS/ Battery systems for very low load situation. *Int. J. Renew. Energy Res. (IJRER)* **2017**, *7*, 844–856.
34. Fazelpour, F.; Soltani, N.; Rosen, M.A. Feasibility of satisfying electrical energy needs with hybrid systems for a medium-size hotel on Kish Island, Iran. *Energy* **2014**, *73*, 856–865. [[CrossRef](#)]
35. Bhattacharjee, S.; Acharya, S. PV–wind hybrid power option for a low wind topography. *Energy Convers. Manag.* **2015**, *89*, 942–954. [[CrossRef](#)]
36. Türkay, B.E.; Telli, A.Y. Economic analysis of standalone and grid connected hybrid energy systems. *Renew. Energy* **2011**, *36*, 1931–1943. [[CrossRef](#)]
37. Thakur, G.; Sharma, K.K.; Kaur, I.; Singh, B. *Cost Analysis of Hybrid Power System Design Using Homer*; Springer: Singapore, 2018; pp. 247–257.
38. Nafeh, A.E. Optimal economical sizing of a PV-wind hybrid energy system using genetic algorithm. *Int. J. Green Energy* **2011**, *8*, 25–43. [[CrossRef](#)]
39. Li, B.; Roche, R.; Miraoui, A. Microgrid sizing with combined evolutionary algorithm and MILP unit commitment. *Appl. Energy* **2017**, *188*, 547–562. [[CrossRef](#)]
40. Abdelhamid, K.; Rachid, I. Techno-economic optimization of hybrid photovoltaic/wind/diesel/battery generation in a stand-alone power system. *Sol. Energy* **2014**, *103*, 171–182.
41. Heydari, A.; Askarzadeh, A. Optimization of a biomass-based photovoltaic power plant for an off-grid application subject to loss of power supply probability concept. *Appl. Energy* **2016**, *165*, 601–611. [[CrossRef](#)]
42. Spyrou, I.D.; Anagnostopoulos, J.S. Design study of a stand-alone desalination system powered by renewable energy sources and a pumped storage unit. *Desalination* **2010**, *257*, 137–149. [[CrossRef](#)]
43. Zahboune, H.; Zouggar, S.; Krajacic, G.; Varbanov, P.S.; Elhafyani, M.; Ziani, E. Optimal hybrid renewable energy design in autonomous system using Modified Electric System Cascade Analysis and Homer software. *Energy Convers. Manag.* **2016**, *126*, 909–922. [[CrossRef](#)]
44. Fazelpour, F.; Soltani, N.; Rosen, M.A. Economic analysis of standalone hybrid energy systems for application in Tehran, Iran. *Int. J. Hydrog. Energy* **2016**, *41*, 7732–7743. [[CrossRef](#)]
45. Oyedepo, S.O.; Uwoghiren, T.; Babalola, P.O.; Nwanya, S.C.; Kilanko, O.; Leramo, R.O.; Aworinde, A.K.; Adekeye, T.; Oyebanji, J.A.; Abidakun, O.A. Assessment of Decentralized Electricity Production from Hybrid Renewable Energy Sources for Sustainable Energy Development in Nigeria. *Open Eng.* **2019**, *9*, 72–89. [[CrossRef](#)]
46. Al Garni, H.Z.; Awasthi, A.; Ramli, M.A. Optimal design and analysis of grid-connected photovoltaic under different tracking systems using HOMER. *Energy Convers. Manag.* **2018**, *155*, 42–57. [[CrossRef](#)]
47. Diemuodeke, E.; Addo, A.; Oko, C.; Mulugetta, Y.; Ojapah, M. Optimal mapping of hybrid renewable energy systems for locations using multi-criteria decision-making algorithm. *Renew. Energy* **2019**, *134*, 461–477. [[CrossRef](#)]
48. Radomes, A.A., Jr.; Arango, S. Renewable energy technology diffusion: An analysis of photovoltaic-system support schemes in Medellín, Colombia. *J. Clean. Prod.* **2015**, *92*, 152–161. [[CrossRef](#)]
49. Ogunjuyigbe, A.S.; Ayodele, T.R.; Akinola, O.A. Optimal allocation and sizing of PV/ Wind/Split-diesel/Battery hybrid energy system for minimizing life cycle cost, carbon emission and dump energy of remote residential building. *Appl. Energy* **2016**, *171*, 153–171. [[CrossRef](#)]
50. Salas, V.; Suponthana, W.; Salas, R.A. Overview of the off-grid photovoltaic diesel batteries systems with AC loads. *Appl. Energy* **2015**, *157*, 195–216. [[CrossRef](#)]
51. Shafiullah, G.M. Hybrid renewable energy integration (HREI) system for subtropical climate in Central Queensland, Australia. *Renew. Energy* **2016**, *96*, 1034–1053. [[CrossRef](#)]

52. Bhandari, B.; Lee, K.T.; Lee, C.S.; Song, C.K.; Maskey, R.K.; Ahn, S.H. A novel off-grid hybrid power system comprised of solar photovoltaic, wind, and hydro energy sources. *Appl. Energy* **2014**, *133*, 236–242. [[CrossRef](#)]
53. Dawood, F.; Shafiullah, G.M.; Anda, M. Stand-alone microgrid with 100% renewable energy: A case study with hybrid solar PV-battery-hydrogen. *Sustainability* **2020**, *12*, 2047. [[CrossRef](#)]
54. Abdul-Wahab, S.; Charabi, Y.; Al-Mahruqi, A.M.; Osman, I.; Osman, S. Selection of the best solar photovoltaic (PV) for Oman. *Sol. Energy* **2019**, *188*, 1156–1168. [[CrossRef](#)]
55. Shaahid, S.M.; Alhems, L.M.; Rahman, M.K. Techno-economic assessment of establishment of wind farms in different provinces of Saudi Arabia to mitigate future energy challenges. *Therm. Sci.* **2019**, *23*, 2909–2918. [[CrossRef](#)]
56. Sami, B.S.; Sihem, N.; Zafar, B.; Adnane, C.; Ahmed, A.E. Performance evaluation of an appraisal autonomous system with hydrogen energy storage devoted for Tunisian remote housing. In Proceedings of the 1st International Conference on Smart Innovation, Ergonomics and Applied Human Factors (SEAHF), Madrid, Spain, 22–24 January 2019; pp. 274–281.
57. Das, M.; Singh, M.A.K.; Biswas, A. Techno-economic optimization of an off-grid hybrid renewable energy system using metaheuristic optimization approaches—case of a radio transmitter station in India. *Energy Convers. Manag.* **2019**, *185*, 339–352. [[CrossRef](#)]
58. Ma, T.; Javed, M.S. Integrated sizing of hybrid PV-wind-battery system for remote island considering the saturation of each renewable energy resource. *Energy Convers. Manag.* **2019**, *182*, 178–190. [[CrossRef](#)]
59. Karmaker, A.K.; Hossain, M.A.; Manoj Kumar, N.; Jagadeesan, V.; Jayakumar, A.; Ray, B. Analysis of Using Biogas Resources for Electric Vehicle Charging in Bangladesh: A Techno-Economic-Environmental Perspective. *Sustainability* **2020**, *12*, 2579. [[CrossRef](#)]
60. Kumar, N.M.; Vishnupriyan, J.; Sundaramoorthi, P. Techno-economic optimization and real-time comparison of sun tracking photovoltaic system for rural healthcare building. *J. Renew. Sustain. Energy* **2019**, *11*, 015301. [[CrossRef](#)]
61. Duffie, J.A.; Beckman, W.A. Design of photovoltaic systems. *Sol. Eng. Therm. Process.* **1991**, *2*, 770–781.
62. Krishan, O.; Suhag, S. Techno-economic analysis of a hybrid renewable energy system for an energy poor rural community. *J. Energy Storage* **2019**, *23*, 305–319. [[CrossRef](#)]
63. Krishan, O.; Suhag, S. An updated review of energy storage systems: Classification and applications in distributed generation power systems incorporating renewable energy resources. *Int. J. Energy Res.* **2018**, *43*, 6171–6210. [[CrossRef](#)]
64. Adefarati, T.; Bansal, R.C. Reliability, economic and environmental analysis of a microgrid system in the presence of renewable energy resources. *Appl. Energy* **2019**, *236*, 1089–1114. [[CrossRef](#)]
65. Ramesh, M.H.; Saini, R.P. Dispatch strategies based performance analysis of a hybrid renewable energy system for a remote rural area in India. *J. Clean. Prod.* **2020**, *259*, 120697. [[CrossRef](#)]
66. Fthenakis, V.M.; Kim, H.C.; Alsema, E. Emissions from photovoltaic life cycles. *Environ. Sci. Technol.* **2008**, *42*, 2168–2174. [[CrossRef](#)]
67. Thomson, R.C.; Harrison, G.P. *Life Cycle Costs and Carbon Emissions of Offshore Wind Power*; ClimateXChange: Edinburgh, UK, 2017.
68. Liu, W.; Sang, J.; Chen, L.; Tian, J.; Zhang, H.; Palma, G.O. Life cycle assessment of lead-acid batteries used in electric bicycles in China. *J. Clean. Prod.* **2015**, *108*, 1149–1156. [[CrossRef](#)]

